Fall 2015

Dynamin Association with Clathrin and Its Physiological Roles at the Golgi and Targeting Mechanism to the Golgi

Shiva Kumar Goud Gadila

DYNAMIN ASSOCIATION WITH CLATHRIN AND ITS PHYSIOLOGICAL ROLES AT THE GOLGI AND TARGETING MECHANISM TO THE GOLGI

A Masters Thesis

Presented to

The Graduate College of

Missouri State University

In Partial Fulfillment

Of the Requirements for the Degree

Master of Science, Biology

By

Shiva Kumar Goud Gadila

December 2015

DYNAMIN ASSOCIATION WITH CLATHRIN AND ITS PHYSIOLOGICAL ROLES AT THE GOLGI AND TARGETING MECHANISM TO THE GOLGI

Biology

Missouri State University, December 2015

Master of Science

Shiva Kumar Goud Gadila

ABSTRACT

Vps1 (Vacuole protein sorting 1), a dynamin-like protein in yeast, is implicated in diverse membrane trafficking pathways and localized to many organelles, including the Golgi. It has been proposed that Vps1 is functionally linked to clathrin heavy chain 1 (Chc1), but the question of how, where, and when they function together remains unknown. Lines of evidence suggest that Chc1 and Vps1 are located at the late Golgi. Therefore, I hypothesized that Vps1 binds to Chc1 and functions together at the Golgi for efficient Golgi-to-endosome membrane trafficking. Using the yeast-two hybrid assay, I present evidence that Vps1 binds to the C-terminal region of the Chc1. Loss of Vps1 resulted in a mislocalization of Chc1, but not Gga1 adaptor, to the late endosome and to the vacuolar rim, suggesting Vps1 is required for Chc1 recruitment to the Golgi. In addition, I found that recruitment of Vps1 to the Golgi requires either the middle or the C-terminal domain of Vps1, but each of these domains showed reduction in the efficiency of targeting to the Golgi. I also found that the mean number of the late Golgi in *vps1* mutant cells was drastically increased, probably because Vps1's involvement in the homotypic fusion at the trans-Golgi network might be affected in those mutant cells. Taken together, my results support the hypothesis that Vps1 functions at the Golgi with Chc1 and provide new insights into the activity of Vps1.

KEYWORDS: Vps1, Chc1, secretory pathway, TGN, endosome

This abstract is approved as to form and content

_____

Dr. Kyoungtae Kim
Chairperson, Advisory Committee
Missouri State University

DYNAMIN ASSOCIATION WITH CLATHRIN AND ITS PHYSIOLOGICAL ROLES AT THE GOLGI AND TARGETING MECHANISM TO THE GOLGI

By

Shiva Kumar Goud Gadila

A Masters Thesis
Submitted to the Graduate College
Of Missouri State University
In Partial Fulfillment of the Requirements
For the Degree of Master of Science, Biology

December 2015

Approved:

_____
Dr. Kyoungtae Kim

_____
Dr. Paul Durham

_____
Dr. Laszlo Kovacs

_____
Dr. Julie Masterson: Dean, Graduate College

ACKNOWLEDGEMENTS

I would like to express the deepest appreciation to my committee chair Dr. Kyoungtae Kim for giving me the opportunity to work in his lab and providing me with his help and guidance in my research. I also want to thank my committee members, Dr. Paul Durham and Dr. Laszlo Kovacs, for their advice and encouragement during my research. In addition, I would like to acknowledge my colleagues Michelle Williams, Katelyn, Hyoeun McDermott, Christopher Trousdale, Bryan Banh, Uma Saimani, Pelin Makaraci, Sara Woodman, John Short, Smock Ashley, and Mariel Delgado Cruz for all of their assistance in my research. Next, I would like to thank the Biology Department and the Graduate College for their financial support. Finally, I would like to thank my family and friends for their support and encouragement.

I dedicate this thesis to my mother.

TABLE OF CONTENTS

LIST OF TABLES

LIST OF FIGURES

INTRODUCTION

Proteins are primary regulators for a diverse range of cellular activities in the cell. In eukaryotes, secretory proteins, such as transmembrane proteins located at the plasma membrane are synthesized in the rough endoplasmic reticulum (RER) and then delivered to the Golgi apparatus via transport vesicles that are coated by COPII (Fig. 1A&B) (Bannykh and Balch, 1997). After a series of chemical modifications, mature proteins are sorted into transport vesicles (TVs) emerging from the trans-Golgi network (TGN). The Golgi-derived TVs are targeted to, via secretory pathways, their final destinations, including the plasma membrane (apical or basolateral membranes in polarized cells) and intracellular organelles like endosomes and the lysosome (Anitei and Hoflack, 2011a). In addition, to retrieve ER and Golgi-resident enzymes, COPI-coated vesicles mediate the retrograde transport from the TGN to earlier Golgi cisternae and to the ER (Fig. 1A&B) (Szul and Sztul, 2011).

Two well-known cargoes for the TGN-to-endosome traffic are a mammalian lysosomal hydrolase containing mannose-6-phospahate (M6P) (Kornfeld, 1992) and a yeast (*Saccharomyces cerevisiae)* carboxypeptidase Y (CPY) (Fig. 1A&B) (Marcusson et al., 1994). Prior to transport to the endosome, these soluble cargoes are physically associated with their corresponding receptors, mannose-6-phosphate receptor (M6PR) and the CPY-receptor Vps10, respectively. The cargo-laden vesicle destined to the endosome is coated by clathrin and its adaptor protein AP1 (Bowers and Stevens, 2005). After the cargo delivery, M6PR and Vps10 are retrieved back to the Golgi by the retromer and sorting nexins from the endosome (Kümmel and Ungermann, 2014;

Marcusson et al., 1994; Seaman, 1997; Seaman et al., 2013). On the other hand, CPY-loaded endosomes mature into late endosomes that fuse with the vacuole to release CPY in the vacuolar lumen (Fig. 1B). Interestingly, a class of proteins, including mammalian lysosomal tyrosinase, are known to be transported directly from early endosomes to the lysosome, and the cargo-carrying vesicle for this traffic is coated by AP-3 and clathrin, thus bypassing the late endosome (Fig. 1A) (Theos et al., 2005). In yeast, AP-3 is only utilized in coating TGN-derived vesicle with the cargo alkaline phosphatase (Fig. 1B), and it was found that the AP-3 coated vesicle is not associated with clathrin and is directly targeted to the vacuole, not passing through the endosomal system (Bowers and Stevens, 2005; Cowles et al., 1997).

Dynamic nature of the Golgi stacks

The Golgi apparatus, consisting of multiple layers of disk-like membrane called cisternae, is involved in packaging and distributing protein cargoes to different cellular organelles (Rabouille and Kondylis, 2007). The eukaryotic Golgi apparatus is subdivided into three classes, *cis*-, *medial*-, and *trans*-Golgi representing discrete stages of maturation (Day et al., 2013). Secretory cargo from the ER enters the Golgi apparatus at *cis* phase of the stack and finally exits from *trans* phase (Farquhar and Palade, 1981). Layers of *trans*-cisterna are transformed into so called trans-Golgi Network (TGN), derived from the last two adjacent *trans*-Golgi cisterna (De Matteis and Luini, 2008; Farquhar and Palade, 1981). The TGN is responsible for the packaging of secretory proteins into transport vesicles and delivering them to different cell organelles like endosomes and vacuoles (Anitei and Hoflack, 2011a; Kang et al., 2011; Mellman and

Simons, 1992). The maintenance of intact structure of these Golgi stacks is assisted by the microtubule system (Hammond and Glick, 2000; Thyberg and Moskalewski, 1999). Thus, the exposure of eukaryotic cells to drugs such as colchicine and vinblastine leads to disassembly of microtubules, which in turn causes disorganization of the Golgi complex, providing evidence of the important role of microtubules in the maintenance of the Golgi complex (Thyberg and Moskalewski, 1985). This feature of Golgi stacks appears to be common throughout the eukaryotic systems (Fig. 1A) (Klumperman, 2011). Furthermore, in mammalian cells multiple Golgi stacks are laterally interconnected to form a compact Golgi-ribbon, located near the centrosome (Wei and Seemann, 2010). However, in other eukaryotes like *Drosophila melanogaster* and the methylotrophic yeast *Pichia pastoris*, Golgi stacks are not interconnected but randomly distributed in the cytoplasm (Prydz et al., 2008). Unlike other eukaryotes, in the budding yeast *Saccharomyces cerevisiae*, Golgi cisternae are not stacked, but rather an individual cisterna is dispersed throughout the cytoplasm (Fig. 1B) (Suda and Nakano, 2012). Some protozoans like *Giardia intestinalis* and *Entamoeba histolytica*, which were previously thought to lack Golgi, are now known to contain Golgi proteins, pointing to the presence of Golgi even in the simplest eukaryotic species (Dacks et al., 2003). Regardless of whether the Golgi apparatus is stacked or dispersed, the cisternae vary in number and its constituents (Papanikou and Glick, 2014, 2009). For example, in *Pichia pastoris* the number of cisterna per stack is as few as 3-4, whereas this number increases up to 20 in some algae species (Day et al., 2013).

Cargo Sorting at the TGN

At the TGN, cargo sorting into specific TVs requires coat proteins, which interact directly or indirectly with sorting signals located in the cytoplasmic domains of these cargoes (Bonifacino and Glick, 2004). Along with the coat proteins, there are several different machineries involved in the process of transport of these vesicles towards the target organelle. The use of advanced imaging techniques like time-lapse fluorescence microscopy and electron tomography has allowed the dynamic observation of these post-TGN transport vesicles in trafficking.

The common sorting machinery at the TGN consists of adaptor proteins (APs), phosphatidylinositols (PIPs), ADP ribosylation factor (ARF), Golgi-localized, γ ear-containing ARF-binding proteins (GGAs), and clathrin the coat protein (Fig. 2) (McNiven and Thompson, 2006). Among these, heterotetrameric APs provide the first line of cargo sequestration specificity (Edeling et al., 2006) by recognizing sorting motifs that are present in the cytosolic domains of the cargo (Bonifacino and Traub, 2003). There are 3 different classes of sorting motifs in these cargo tails, which are decoded by adaptor proteins (AP-1, AP-2, AP-3, and AP-4), and thereby segregating cargoes into transport vesicles (Anitei et al., 2010c). Firstly, at the TGN, AP-1 associates with two types of sorting motifs, a tyrosine-based Tyr-X-X-Ø motif and a dileucine-based [Asp-Glu]X-X-X-Leu[Leu-Ile] motif, which are present in the cytosolic tails of cargoes destined for endosomal/lysosomal compartments (Bonifacino and Traub, 2003). The tyrosine-based motif is present in the cytosolic tail of mannose-6-phosphate receptor (M6PR), shuttling back and forth between the TGN and endosomes for delivering newly synthesized acid hydrolases to the endosome (Ghosh et al., 2003). Similarly, the budding

yeast has a transmembrane protein, Vps10, which delivers carboxypeptidase Y (CPY) to the endosome via a tyrosine-based signal (YSSL80) homologous to the sorting signal of the mammalian M6PR (Cooper and Stevens, 1996). At the plasma membrane, the Asn-Pro-X-Tyr motif, which is present in the cytoplasmic tails of the insulin receptor and epidermal growth factor (EGF) receptor is decoded by AP-2 (Robinson, 2004).

The phospholipid phosphatidylinositol-4-phospahte (PI4P) is highly enriched at the TGN. The synthesis of PI4P requires a phosphorylation of phosphatidylinositol by phosphatidylinositol-4-kinase (PIK1) (Wiedemann et al., 1996). A clue to the critical role of PI4P in the TGN-to-endosome traffic was discovered from studies of the secretory pathway in budding yeast in which a yeast strain with a temperature-sensitive mutation in the PIK1 displayed a severe defect in cargo exit from the Golgi (Strahl et al., 2005). In addition, PI4P is also involved in the recruitment of AP-1 and GGAs to the TGN (Wang et al., 2003). At the plasma membrane, phosphatidylinositol 4,5-bisphosphate (PIP_2) is enriched, which binds to AP-2 (Puertollano, 2004). Even though these PIPs are important in the protein sorting process, they alone do not provide specificity without small GTPases. The adenosine diphosphate ribosylation factor (ARF) family of small GTPases plays an important role in regulating vesicular traffic (D'Souza-Schorey and Chavrier, 2006). ARF1, a family member of ARF, regulates in its active form the recruitment of AP-1 to the TGN, indicating ARF1 along with PI4P is involved in the regulation of recruitment of AP-1 to the TGN (Puertollano, 2004). ARF1 also regulates the recruitment of the PI4K/Pik1 to the Golgi essential for the production of the PI4P. Mutational analysis in yeast revealed that there was 40% reduction in the levels of PI4P in *arf1*Δ cells (Audhya et al., 2000; Santiago-Tirado and Bretscher, 2011).

A second family of adaptor proteins at the TGN consists of GGAs, which are monomeric proteins containing C-terminal domain homologous to that of AP-1 subunit and function along with the AP-1 (Bonifacino, 2004). Similar to AP-1, the recruitment of GGAs to the TGN depends on ARF1 (Donaldson et al., 2005). However, GGAs-mediated protein sorting varies from AP-1 in that GGAs bind to unique Asp-X-X-Leu-Leu motif (Fig. 2B&C) (McNiven and Thompson, 2006). These GGAs are also known to interact with ubiquitinated cargo, such as the cation-independent and cation-dependent M6PR, via their VHS (Vps27, Hrs and STAM) and GAT domains, which was characterized by pull-down and two-hybrid assays (Puertollano and Bonifacino, 2004). In particular, the GAT domain of the GGA proteins is implicated in sorting of the ubiquinated Gap1 amino acid transporter from the TGN to endosomes (Scott et al., 2004).

The clathrin coat assembles into cage-like lattices around the transport vesicles, forming clathrin coated vesicles. Clathrin recruitment to the TGN is dependent on AP-1, which is recruited to the TGN by ARF1 (Donaldson et al., 2005). GGAs also contribute to the recruitment of clathrin to the TGN via the interaction between the clathrin-box like sequences in GGAs and the N-terminal domain of clathrin heavy chain (Puertollano et al., 2001). Therefore, GGAs along with AP-1 play a key role in the assembly of clathrin at the TGN. Lipid-binding proteins such as Epsin-related (EpsinR), which has one of two motifs, the Epsin N-terminal homology/AP180 N-terminal homology (ENTH/ANTH) domain (Duncan and Payne, 2003) and the Bin-amphiphysin-Rvs161/167p (BAR) domain (Peter et al., 2004) are also involved in clathrin coat vesicle formation at the TGN (Duncan and Payne, 2003).

Membrane Tubulation, Scission and Transport

Membrane curvature is the first step in the biogenesis of a transport vesicle. At the TGN, the membrane curvature process is induced by coat proteins, such as clathrin, which functions with adaptor proteins. Along with the adaptor proteins, clathrin also works with accessory proteins containing ENTH/ANTH domains, which bind PIPs and penetrate the outer membrane of membrane bilayer and induce membrane bending (Fig. 3A) (Anitei and Hoflack, 2011b). After the initial membrane deformation process, actin polymerization provides the required forces for the formation of the invaginated precursor tubule towards the cytoplasm. At the TGN, F-actin elongates towards the neck of the membrane curvature, with barbed ends of actin filaments situated at the vicinity of the neck. The polarized growth at the barbed ends provides a pushing force on the membrane to induce an established tubular structure (Fig. 3B) (Anitei et al., 2010a). It is known that dynamic actin assembly is mediated by the Arp2/3 complex and formins upon internal and external signals (Suetsugu, 2009). In particular, Arp2/3 complex-mediated actin assembly is stimulated by WASP (Wiskott-Aldrich Syndrome Protein) family members (Rottner et al., 2010). WAVE/SCAR complex, a WASP family member, is recruited by clathrin/AP-1 coats at the TGN, for the activation of Arp2/3 complex-mediated actin polymerization that drives precursor tubule formation (Anitei et al., 2010b). For the precursor tubule formation, myosin motor proteins, such as Myo1b, walk along with the F-actin at the TGN (Coudrier and Almeida, 2011). Myo1b recruitment to the Golgi membrane depends on its pleckstrin homology domain that binds to PI4P (Vicinanza et al., 2008). The head of myo1b moves on F-actin in a positive-directed

manner and generates the power stroke, while the tail pulls the membrane, leading to the formation of precursor tubule (Fig. 3C) (Dippold et al., 2009).

Clathrin coat formation along with the actin polymerization creates the necessary membrane curvature for the recruitment of BAR domain containing proteins that sense the characteristic concave shape of the invaginated membrane (McMahon and Gallop, 2005). It is well-known that BAR domains are able to dimerize to form a banana-shaped arc (Frost et al., 2000). The concave surface of the arc has several positively charged amino acid residues that bind through electrostatic interactions to negatively charged phospholipid-containing membranes to assist membrane curvature process through scaffolding (Yu and Schulten, 2013). The electrostatic interaction between BAR domains and the phospholipid was drastically inhibited by replacing two positively charged residues with negatively charged glutamate, leading to defects in membrane tubulation process *in vitro* (Peter et al., 2004). However, direct evidence for BAR-induced intracellular membrane deformation *in vivo*, is currently lacking as it is difficult to access the heterogeneous phospholipid compositions at each membrane (Suarez et al., 2014). In addition to their role in membrane deformation and stabilization, BAR domain proteins bind to WASP family members and support F-actin polymerization, which is required for the tubule elongation (Ferguson et al., 2009). It was reported that Arfaptin-1 consisting of a N-BAR domain is involved in the biogenesis of transport vesicle at the TGN (Gehart et al., 2012), whereas, Amphiphysin, an N-BAR domain containing protein, binds to and is involved in the tubulation process at the plasma membrane (McMahon and Gallop, 2005).

Microtubule-associated motor proteins are also involved in the extension of the membrane tubulation as evidenced by the presence of enriched kinesins at the tips of the emerging tubule at the TGN (Almeida et al., 2011; Anitei and Hoflack, 2011b; Polishchuk et al., 2003). Similar to myosin, kinesin recruitment onto membranes involves adaptor proteins, PIPs, SNXs, and GTPases (Hirokawa et al., 2009). At the TGN, kinesin (KIF13A) associates with beta 1-adaptin, a subunit of the AP-1 adaptor protein complex (Nakagawa et al., 2000). This plus-end directed kinesin move along microtubules and exert forces on to the membrane to which they are attached, leading to a tubule elongation (Fig. 3D) (Koster et al., 2003; Kreitzer et al., 2000; Roux et al., 2002). In light of finding that the microfilament system is mainly implicated in nascent or precursor tubule at the TGN and that kinesins are only located at the tubule tip, it is likely that the kinesin-mediate tubule elongation is preceded by the actin-myosin's role at TGN (Almeida et al., 2011). However, the precise spatiotemporal recruitment process of machineries required for producing the force for the initial and further tubule elongation is poorly understood.

Following the tubulation process of the membrane, the final mechanism for the release of the transport vesicles is the scission process. In mammals, dynamin-2 is implicated in its role as a molecular pinchase at the TGN (Weisz and Rodriguez-Boulan, 2009). Dynamin family members are found throughout the eukaryotic system, and members of dynamin superfamily are subdivided, based on functional characteristics, into classical dynamins and dynamin-related or dynamin-like proteins (DRPs or DLPs) (Ramachandran, 2011). Classical dynamins consists of 5 different domains: an N-terminal GTPase, or G-domain, an α-helical stalk, Pleckstrin Homology (PH) domain,

bundle signaling element (BSE), and a C-terminal proline-rich domain (PRD) (Chappie and Dyda, 2013; Cocucci et al., 2014). The stalk domain self-assembles in a criss-cross fashion, which is essential for formation of dynamin dimers and consequently an oligomer (Gao et al., 2010). The interaction between G-domains positioned in adjacent rungs of the dynamin helix facilitates GTPase activity. It is reported that dimers and tetramers of dynamin forms in the solution, prior to their recruitment to the membrane via using the PH domain *in vitro* (Chappie and Dyda, 2013). Dynamin oligomerization occurs along the neck of the invaginating tubule (Mettlen et al., 2009), which allows G domains to be optimally situated for interaction between them. GTP binding and hydrolysis at the G domain across the dynamin oligomer results in production of increased force to generate greater strain on the membrane neck, leading to a membrane constriction (Schmid and Frolov, 2011). The current models for the dynamin polymer shows that an inner luminal diameter of the neck of an invaginating tubule is about ~7 nm before constriction, whereas the diameter decreases to 4nm after dynamin-mediated constriction (Chappie and Dyda, 2013; Chappie et al., 2010). DRPs or DLPs contain three of those five domains present in classical dynamins: the N-terminal GTPase domain, middle domain, and the C-terminal GED domain (Smaczynska-de Rooij et al., 2012). Without exception, human dynamin related proteins, such as DRP1 and OPA1, have a PH domain along with GTPase, middle, and GED domains (Praefcke and McMahon, 2004). There are 3 different DRPs in yeast, Mgm1, Dnm1, and Vps1. These DRPs are involved in several different cellular processes like mitochondrial fission by Dnm1, mitochondrial fusion by Mgm1, and vacuolar fission by Vps1 (Chappie and Dyda, 2013; Praefcke and McMahon, 2004). DRPs, therefore, carry out membrane scission

process similar to those of classical dynamins. The GTP hydrolysis-dependent conformational changes were observed for the yeast mitochondrial dynamin-like protein Dnm1 (Mears et al., 2011), and this change was not seen upon addition of the non-hydrolyzable GTP analog GMPPCP, suggesting the G domain may play an important role in mitochondrial fission (Chappie et al., 2011). It was suggested that Vps1 works together with clathrin to pinch off vesicles from the late Golgi in the budding yeast (Conibear and Stevens, 1995) on the basis of the observation that Vps1 and clathrin genetically interact (Bensen et al., 2000). In agreement with this notion, Vps1 showed partial overlap with a late Golgi marker (Lukehart et al., 2013), suggesting that it functions at the late Golgi. However, a direct physical interaction between clathrin and Vps1 at the TGN has not been documented.

Interestingly, recent evidence showed a functional link of dynamin and DLPs with actin at the plasma membrane for efficient endocytosis. Dynamin was found to be recruited to the invaginated membrane where it binds to actin, which triggers increased recruitment and stabilization of dynamin oligomeric structures (Grassart et al., 2014; Taylor et al., 2012). The interaction with actin appears to be conserved in yeast Vps1, as manifested by both Vps1 interaction with actin filaments and vps1-mediated actin bundle formation. More importantly, cells expressing a mutated Vps1 protein lacking its ability to bundle actin filaments displayed a significant endocytic defect (Palmer et al., 2015), indicating Vps1 interaction with actin is functionally relevant. The question of whether Vps1 functions together with actin at the TGN has not been well addressed.

Golgi-derived vesicles are transported towards endosomes via a microtubule dependent pathway (Anitei et al., 2010c). These transport vesicles from the TGN are

connected to molecular motors, kinesin13A (Delevoye et al., 2009; Fölsch et al., 1999; Nakagawa et al., 2000) or kinesin 5B (Schmidt et al., 2009) that mediate trafficking along microtubules for their delivery to the endosome. Kinesin 13A was found to interact directly with AP-1 subunits (Fölsch et al., 1999; Nakagawa et al., 2000), while kinesin 5B interacts indirectly with AP-1 through Gadkin, an accessory protein that links AP-1 to the kinesin (Schmidt et al., 2009). The recruitment of these kinesin motor proteins on to microtubules is dependent on the conformational changes of Rab GTPases to an active form (Stenmark, 2009).

Vesicle Tethering and Fusion

Following the budding process from the TGN, a transport vesicle moves towards the target organelle, such as endosomes and the vacuole, for fusion, which is required for the final delivery of cargo. This fusion process is preceded by tethering, which is the initial interaction between vesicle and the target organelle at the distance, followed by a closer interaction or a docking that leads to the fusion between them (Brown and Pfeffer, 2010). Tethering at the endosome is mediated by Class C core vacuole/endosome tethering (CORVET) (Fig. 4A), a multiple protein complex consisting of 6 Vps (vacuolar protein sorting) proteins: Vps11, Vps16, Vps18, Vps33, Vps3, and Vps8 (Peterson and Emr, 2001). Of these the first four proteins are called the class C proteins, which are also shared with the tethering complex HOPS found at the vacuole (Ostrowicz et al., 2010). The remaining two subunits, Vps3 and Vps8, mediate the binding of the CORVET complex with its upstream regulator Rab5 GTPase, a functional homolog of yeast Vps21 located at the endosome (Markgraf et al., 2009; Peplowska et al., 2007). At one end, this

CORVET complex associates with SNAREs on Golgi-derived vesicles, and the other end is physically linked to Rab5 on the endosome, there by serving as a bridge between these two approaching membranes (Ostrowicz et al., 2010; Peterson and Emr, 2001). A pulse-chase radiolabeling assay revealed that temperature-sensitive mutants of *vps11, vps16, vps18,* and *vps33* displayed at non-permissive temperatures exhibited the abnormal accumulation of the premature CPY containing Golgi-derived vesicles in the cytoplasm (Peterson and Emr, 2001; Subramanian et al., 2004), highlighting the significance of CORVET in cargo transport toward the vacuole. Along with its function in the tethering of Golgi-derived vesicles with endosomes, CORVET is also involved in the homotypic fusion of early endosomes (Kümmel and Ungermann, 2014).

In addition to CORVET complex, the Rab effectors early endosome antigen 1 (EEA1) and Rabenosyn-5-Vps45 complex are required for the successful tethering and fusion of the Golgi-derived vesicle with the early endosome and also for the homotypic fusion between endosomes (Fig. 4A) (Balderhaar and Ungermann, 2013; Ohya et al., 2009; Sriram et al., 2003). Firstly, EEA1, is a long coiled-coil protein consisting of N-terminal C_2H_2 (2 cysteines and 2 Histidines), which is a Zinc finger domain (ZF) that binds to Rab5 with high affinity. The C-terminus of EEA1 comprises of FYVE domain that binds to phosphatidylinositol-3-phosphate (PI3P) at the early endosome. The yeast two-hybrid studies revealed that Vac1 the yeast homolog of EEA1 physically interacts with Vps11 subunit of CORVET complex (Peterson and Emr, 2001), and fluorescence microscopy analysis revealed that both Vps11 and EEA1 localize at the early endosomes in mammalian cells (Chirivino et al., 2011). A pulse-chase radiolabeling assay revealed that yeast strains lacking Vac1 have blockage in the trafficking of vacuolar hydrolases

CPY, protease A, and protease B. In addition, strains lacking Vac1 accumulated a 40-60nm vesicle population, which were spatially not overlapping with endosomal compartments, indicating a tethering defect mediated by Vac1 involvement upon its loss, a necessary prerequisite step for the fusion at the endosome (Webb et al., 1997).

The second Rab effector, Rabenosyn-5 also contains a N-terminal C_2H_2 ZF that binds to Rab5 and FYVE domain binding to PI3P, whereas, C-terminal domain represents a further binding site for Rab5, allowing Rabenosyn-5 to act as a tether (Mishra et al., 2010). This Rabenosyn-5 forms a complex with Vps45, a SM (Sec1 and Munc18) family protein, which acts as a chaperone that links the Rab and SNARE machinery (Morrison et al., 2008). Mutational analysis in yeast demonstrated that CPY containing Golgi-derived vesicles are accumulated in the cytoplasm of Vps45 knock out cells (Burd et al., 1997). These findings provide evidence of the significance of these Rab5 GTPase effectors involvement in the tethering and fusion of the Golgi-derived vesicles with endosomes (Ostrowicz et al., 2010; Peterson and Emr, 2001).

Recruitment of the CORVET complex and EEA1 on the endosome depends on the activation of their upstream regulator Rab5, mediated by the Rab5 GEF, Rabex-5. Sequencing of mammalian Rabex-5 displayed homology to the yeast protein Vps9 whose intrinsic tethering function at the endosome is conserved (Bröcker et al., 2010; Horiuchi et al., 1997). It is important to note that a loss of Rab GEF or Rab/Ypt displays partial disruption of CORVET targeting to the endosome, whereas the targeting of the EEA1 homolog Vac1 toward the endosome was completely disrupted, suggesting that Vac1 targeting is strictly depending on active Rab5, but not CORVET (Cabrera et al., 2013).

The closer interaction or docking of the Golgi-derived vesicle with the endosome requires tethering factors and SNAREs. Mechanistically, tethering factors interact with multiple structural motifs in SNAREs (Fig. 4B) (Hong and Lev, 2014). Generally, SNARE motif is located in the cytosolic domain of the SNAREs (Fasshauer et al., 1998). For example, Vps33, a subunit of CORVET complex acting as SM (Sec1 and Munc18) family protein, binds to the endosomal SNARE motif of the yeast syntaxin Pep12 to facilitate SNARE complex formation (Subramanian et al., 2004).

SNAREs are recognized as key components of protein complexes that drive membrane fusion (Fig. 4C). Around 36 distinct SNAREs are known in mammals (Hong, 2005), whereas, yeast has 24 different SNAREs, localized to distinct intracellular compartments along the secretory and endocytic pathways (Jahn and Scheller, 2006). Initially, SNAREs were classified as v- and t-SNAREs based on their subcellular localizations, vesicles and target organelles, respectively. Later, these SNAREs were divided into R- and Q- SNAREs based on the presence of highly conserved residues, R (arginine) and Q (glutamine), respectively (Malsam and Söllner, 2011). A R- or v-SNARE on the vesicle interacts with three Q- or t-SNAREs on the target membrane forming a hetero-tetrameric *trans*-SNARE complex, which is also termed as SNAREpins. This SNAREpin is formed in a zipper-like manner starting at the amino-terminal, which is at distal end and moving towards the carboxy-terminal, proximal region of the SNARE (Pobbati et al., 2006). In mammals, typically SNARE complex consists of Qa- (syntaxin 7), Qb- (Vti1a), and Qc- (syntaxin 8) SNAREs on the target endosomal membrane, and R-SNARE (Ykt6) on the Golgi-derived vesicle for a heterotypic fusion (Hong, 2005; Pryor et al., 2004). In yeast, heterotypic fusion is mediated by SNARE complex

consisting of 3 t-SNAREs, Pep12p (Q_a), Vti1p (Q_b), Syn8p (Q_c) and a v-SNARE Ykt6p (R) (Dilcher et al., 2001; Kweon et al., 2003; Lewis and Pelham, 2002). A growing body of evidence is suggestive that these 4 specific or cognate SNAREs are directly involved in the successful fusion of Golgi-derived vesicle at the endosome, while non-cognate t- and v-SNAREs have very little potency to fuse (Furukawa and Mima, 2014; Parlati et al., 2002). The fully assembled post-fusion *cis*-SNARE complex acts as a substrate for SNAPs (soluble NSF attachment factors), which in turn recruits the hexameric ATPase NSF (N-ethylmaleimide sensitive factor) (Whiteheart et al., 1993). ATP hydrolysis by NSF dissociates the SNARE complexes resulting in largely unstructured SNARE proteins, which can be recycled for further rounds of transport (Mayer et al., 1996). In conclusion, membrane fusion is driven by a protein assembly (v-/t- SNARE complex assembly), and ATP hydrolysis is required to disassemble the SNAREs (Malsam and Söllner, 2011).

Future Research Trends

Despite significant progress in understanding the cargo sorting at the TGN, there still exists a plethora of unanswered questions regarding how a cargo-loading site is initially selected prior to cargo segregation and what signaling cascade(s) directs this specific process and afterward. The precise spatiotemporal/biochemical recruitment mechanism of several classes of proteins, which act in this step-by-step event occurring at the TGN, is awaiting further investigation. An important question that has not been well addressed is how cargo-loading machineries at the TGN achieve a successful coordination of cargo-loading speed with the rate of clathrin-coated pit maturation, which appears to be required for making the full-grown vesicle where a sufficient quorum is

reached. A mature cargo-laden vesicle leaves the TGN for cargo delivery to the final destination, and in this regard, vesicle pinching-off by a scission complex must precede the delivery. Though a growing body of evidence points to the implication of mammalian dynamin 2 and yeast Vps1 in the scission event occurring at the TGN, yet the field awaits further direct evidence to support this model. In conjunction with this, tentative collaborative roles of known and unidentified dynamin binding partners, which could regulate positively the membrane constricting role of the pinchase dynamin, should be further explored. Microfilament and microtubule systems, as has been the case, are proven to be involved in secretory vesicle budding, pinching-off, and traffic, but precise functional collaboration mechanisms for these events have remained elusive. A further understanding of the molecular and cellular mechanisms underlying the secretory pathway may be crucial in the treatment of many human diseases like Acute myeloid leukemia (caused by defect in the formation of clathrin-coated pit), Charcot-Marine-Tooth disease (by defect in microtubular transport of synaptic vesicles), Dent's disease (by defects in post-Golgi transport to cell surface), I-cell disease (by defects in M6P addition to lysosomal enzymes), and Wiskott-Aldrich Syndrome (by flaws in WASP regulation of actin cytoskeleton) (Howell et al., 2006).

HYPOTHESIS AND GOALS

The present study reveals the functional relationship between Vps1 and clathrin heavy chain 1 (Chc1) in the budding yeast *Saccharomyces cerevisiae*. On the basis of a previous finding of genetic interaction between Vps1 and Chc1 (Bensen et al., 2000), I hypothesized that Vps1 and Chc1 physically interact with each other and function in a collaborative manner for the traffic from the Golgi to endosomes. To test this possibility, I have used standard techniques of molecular biology, genetics, and cell biology, including the yeast two-hybrid assay, gene cloning and expression, and confocal fluorescence microscopy. My thesis research aims fall into the following three areas.

1) Study a possible direct interaction between Vps1 and Chc1 to provide the first evidence that they function together within the cell.

2) Characterize and quantitate abnormal Golgi phenotypes in cells lacking Vps1. If Vps1 plays an important role in the Golgi-to-endosome traffic, the loss of Vps1 would lead to noticeable Golgi defects such as in its morphology and abundance.

3) Examine the biochemical targeting mechanism of Vps1 to the Golgi. The field of membrane trafficking would benefit from a better understanding of Vps1 recruitment to diverse membrane-bound organelles, including the Golgi.

The result and discussion sections of this thesis provide novel findings regarding the targeting mechanism of Vps1 to the Golgi and evidence of a direct interaction between Vps1 and Chc1, supporting the notion that both proteins function together within the cell. The increase in the number of late Golgi in *vps1* mutant cells indicates the involvement of Vps1 in the maintenance of Golgi structure.

MATERIALS AND METHODS

Yeast Strain Construction and Media

Yeast strains used in this study are listed in Table 1. Yeast strains expressing Chc1-GFP and Gga1-GFP were constructed by integration of GFP sequence at the 3' end of gene of interest using homologous recombination, as previously described (Kim et al., 2006; Longtine et al., 1998; Nannapaneni et al., 2010). In order to generate gene deletion strains, such as *vps1*Δ cells, wild type cells were transformed with PCR products carrying a disruption construct as described previously (Longtine et al., 1998). KKD 0190 (mRFP-Vps1) and KKD 0191 (mRFP-Sft2) plasmids were constructed as follows. The *VPS1* and *SFT2* sequences amplified by PCR from BY4741 genomic DNA were flanked with EcoRI and XhoI sites at the 5' and 3' ends, respectively. The amplified fragment was cloned into the EcoRI-XhoI sites of the pOK489 plasmid (Obara et al., 2013), which contains the mRFP-Cps1, to replace the *CPS1* gene with *VPS1* and *SFT2* genes, thereby producing KKD 0190 and KKD 0191 plasmids. Yeast transformants that harbor the corresponding plasmid were grown on selective plates and were exposed to confocal microscope (See the section "Fluorescence microscopy"). Positive transformants were then collected and grown in standard synthetic defined (SD) liquid medium lacking nutrients required to maintain selection of auxotrophic markers from the plasmids. The plasmids encoding DsRed-FYVE, GFP-PH FAPP1, mRFP-Sft2, and mRFP-Vps1 were introduced into yeast strains by following the one-step transformation protocol (Chen et al., 1992), and grew on corresponding selective media plates. Resulting transformants on

selective plates were screened by confocal microscopy. All plasmids used or constructed in this study are listed in Table 2.

Fluorescence Microscopy

Fluorescently labeled cells were visualized either using a spinning confocal (with Yokogawa CSUX1 spinning disk head, a 100X magnification, numerical aperture (NA) 1.4, PlanApo oil objective, and ImagEM cameras) or a conventional fluorescence microscope (Orca camera). All images were taken using oil immersion at 100X magnification. Simultaneous two-color imaging was done using an image splitter to separate red and green emission signals. In all cases, fluorescent samples were focused at the equatorial plane of the cells, and exposure was set to 100ms for all images, unless otherwise indicated.

Construction of Bait and Prey plasmids and Yeast-Two Hybrid Screening

For the Yeast Two-Hybrid screening method, I used In-Fusion® HD Cloning Kit User Manual from Clontech. Briefly, purified yeast genomic DNA served as a template to amplify the full length DNA sequence of Vps1, three fragmented domains of Vps1 (the GTPase, the middle, and the GED domain), full length of Chc1 (clathrin heavy chain 1), and fragmented domains of Chc1 (N-terminal domain, distal leg, and proximal leg). The amplified PCR products of Vps1 and different fragments of Vps1 were inserted into the EcoRI and BamHI sites of the bait plasmid (pGBKT7), located downstream of the *GAL4* DNA-binding domain (BD) sequence. Similarly, Chc1 and fragmented sequences of Chc1 were inserted into the multi-cloning site of the prey plasmid (pGADT7), located

downstream of *GAL4* DNA-activation domain (AD) sequence. Cloned bait and prey vectors were introduced into Y2H Gold (KKY 1254) and Y187 (KKY 1255) strains, respectively. The cells were grown on corresponding selective media plates. The transformants were incubated at 30^{o}C for 3 days, and colonies were screened using colony PCR. Positive bait and prey colonies were then mated following the manufacture's protocol, Matchmaker Gold Yeast Two-Hybrid System User Manual. The mated culture was plated onto stringent media, lacking tryptophan and leucine (SD/-Trp/-Leu; DDO).

Spotting assays were then performed to determine strength of protein-protein interactions between bait and prey proteins. For this, cells were grown in 3 ml DDO (SD/-Trp/-Leu) at 30^{o}C for 2 days. Then, cells were serially diluted by a factor of 3 in a 96 well plate, and were spotted onto DDO, TDO (SD/-Leu/-Trp/-His), and QDO (SD/-Trp/-Leu/-His/-Ade) agar plates that were grown at 30^{o}C for 3 days. The intensity of the spotted cells on the selective media plates was determined to reveal the strength of interaction between bait and prey proteins.

CMAC Labeling of Yeast Vacuole Membranes

CMAC staining of vacuoles was done by incubating cells with CellTracker Blue™ CMAC (7-amino4chloromethylcoumarin, Molecular Probes Inc.) as previously described (Hayden et al., 2013). The stained cells were then subjected to microscopic analysis.

Statistical Analysis

Quantification of average number of Gga1-GFP puncta in WT and *vps1*Δ cells was carried out by counting, at random, a number of cells in a field of view (n = 30 cells). After the data was gathered, the average of each of the three trials was taken and standard deviation was determined. Similarly, the percentage colocalization between Vps1 and its fragments with Gga1-GFP was determined by counting the RFP puncta that showed colocalization with GFP (n = 30 cells). To analyze if there was a significant difference in the increase of number of GFP-PH FAPP1 puncta between WT and *vps1*Δ cells, two-tailed t-tests were performed.

RESULTS

Domains of Chc1 Shows Physical Interaction with Domains of Vps1

Previously, it was reported that haploid yeast cells harboring the temperature sensitive allele of *CHC1* and *VPS1* showed genetic interaction, indicating a functional connection between these two proteins (Bensen et al., 2000). Additionally, Vps1 showed spatial overlap with a late Golgi marker (Lukehart et al., 2013), suggesting that Vps1 functions at the late Golgi. Given proteins that function together would physically interact with one another, the possibility of Vps1 interaction with Chc1 was tested using the yeast two-hybrid assay. Briefly, the full-length *VPS1* DNA sequence was cloned into the bait vector pGBKT7 to construct pGBKT7-Vps1, and the full-length of *CHC1* sequence was inserted into the prey vector pGADT7 to construct pGADT7-Chc1. Diploid cells harboring both pGBKT7-Vps1 and pGADT7-Chc1 were applied on TDO (SD/-His/-Leu/-Trp) and QDO (SD/-His/-Leu/-Trp/-Ade) plates (Figure 5). Yeast cells co-expressing p53 and SV40 large T antigen were used as a positive control (Figure 5, row 2), and cells co-expressing p53 and Lamin were used as a negative control (Figure 5, row 1). As was the case for the positive control experiment, cells that co-express Vps1 and Chc1 grew on TDO plates (Figure 5, row 5), indicating that Vps1 physically interacts with Chc1 in vivo.

Vps1 is composed of three domains, including the N-terminal GTPase, the middle (or MID) and the C-terminal GED (GTPase Effector Domain) (Praefcke and McMahon, 2004). To map the domain of Vps1 that binds to Chc1, each Vps1 domain was fused with BD in the bait vector. The same positive and negative controls were used to confirm the validity of the experiment. It was found that all three domains of Vps1 (GTPase, Middle

and GED) displayed high affinity binding to the Chc1, as evidenced by growth on TDO and also QDO plates (Figure 5, rows 6-8). Similarly, to map the specific domain of Chc1 that interacts with the specific domain of Vps1, I made 3 fragments of Chc1, including a N-terminal fragment consisting of 494 aa, a distal fragment (495-1073 aa), and a fragment consisting of both proximal domain and trimerization domain (1074-1654 aa). It was found that the N-terminal domain (1- 494 aa) and the distal domain fragment (495-1073 aa) displayed no growth on TDO and QDO plates, indicating no binding of these fragments of Chc1 with Vps1 (Figure 6, A&B). However, the proximal domain and trimerization fragment consisting of 581 aa (1074-1654) showed higher binding affinity with the full-length of Vps1, N-terminal GTPase and C-terminal GED domains of Vps1 (Figure 7). Taken together, these data provide evidence that the N-terminal GTPase and the C-terminal GED domains of Vps1 interact with the C-terminal domain of Chc1 *in vivo*.

Subcellular Localization of the Golgi Adaptor Protein Gga1 in *vps1*Δ Cells

Previously, results from the Kim Lab has shown that loss of Vps1 led to the mislocalization of the Chc1 to the late endosome and the vacuole (data not shown). I therefore further extended my study to check the subcellular localization of another late Golgi factor, such as adaptor protein (Gga1) and Sft2, in *vps1*Δ cells. The reason behind the investigation of Gga1 localization in this condition is that recruitment of clathrin to the Golgi membrane is partly dependent on the adaptor proteins, Gga1 and Gga2. These adaptor proteins are involved in the transportation of the cargo from the TGN to the endosomal system (Ghosh et al., 2003; Scott et al., 2004). I genomically tagged the GFP

sequence to the C-terminal of *GGA1* in WT (Wild type) and *vps1*Δ cells that also express DsRed-FYVE, a fluorescent endosome marker. FYVE finger domains are able to bind PI(3)P, enriched in the endosomal membrane (Burd and Emr, 1998; Gillooly et al., 2000), and thus fluorescent DsRed-FYVE can serve as a fiduciary endosome marker. Gga1-GFP puncta were not found to be colocalized with DsRed-FYVE in both WT and *vps1*Δ cells (Figure, 8), indicating that the adaptor protein Gga1 is not mislocalized to the late endosomal compartment.

I next tested the localization of a late Golgi marker, Sft2. Interestingly, mRFP-Sft2 in *vps1*Δ cells was located to the vicinity of CMAC-labelled vacuole, suggesting a mistargeting of mRFP-Sft2 from the late Golgi to the endosomal system (Figure, 9A). It was obvious that in WT cells mRFP-Sft2 displayed a high level of colocalization to the Golgi marked by Gga1-GFP, whereas in *vps1*Δ cells mRFP-Sft2 was not colocalized with the Golgi, suggesting the possible mislocalization of mRFP-Sft2. (Figure, 9B).

Loss of Vps1 Leads to Increase in the Number of Late Golgi

During the investigation of Gga1-GFP localization in relation with endosomal compartments, I found that there was an increase in the number of Gga1-GFP puncta in *vps1*Δ cells compared to that of WT cells. Upon quantification, the average number of Gga1-GFP puncta in wild type (WT) cells was 4.07 (± 0.67), while the average number of Gga1-GFP puncta in *vps1*Δ cells was 5.8 (± 1.20) (Figure, 10).

To further support my observation with Gga1-GFP counting, I examined the number of late Golgi labeled with another late Golgi marker, GFP-PH FAPP1, in *vps1*Δ cells and *vps1* GTPase mutant cells ($vps1^{K42E}$, $vps1^{S43N}$, and $vps1^{G315D}$). Four-phosphate-

adaptor protein 1 (FAPP1) contains the pleckstrin homology (PH) domain, and therefore, GFP-fused PH binds PI (4)P at the Golgi (Dowler et al., 2000), serving as a fluorescent marker. As expected, we found that there was an increase in the number of GFP-PH FAPP1 by twofold in *vps1*Δ and *vps1* GTPase mutant cells compared to WT cells (Figure, 11) with the average number of GFP-PH FAPP1 puncta in 2 different WT strains (KKY 1395 and KKY 1400) being 5.54 (± 1.641) and 6.32 (± 1.91), respectively. Two different *vps1*Δ strains (KKY 0751 and KKY 1404) showed slightly different average numbers of GFP-PH FAPP1 puncta with 8.84 (± 2.359) and 11.52 (± 2.85), respectively. Similarly, *vps1* GTPase mutant cells (KKY 1391, KKY 1393, and KKY 1402) contained 9.88 (± 3.26), 9.74 (± 2.82), and 10.66 (± 3.20) puncta of GFP-PH FAPP1, respectively. Taken together, the results support the notion that the loss of Vps1 leads to an increase in the number of late Golgi.

Vps1 Targeting Mechanism to the Late Golgi

Vps1 is implicated in diverse membrane trafficking pathways and is localized to many organelles, including the plasma membrane, endosome, vacuole, Golgi, and peroxisome (Williams and Kim, 2014). However, its targeting mechanism to each organelle is poorly understood. To investigate the Vps1 targeting mechanism to the Golgi, I have constructed yeast strains that express Gga1-GFP, which is a fiduciary fluorescence marker for the Golgi. Into these strains I introduced each of the following 5 Vps1 expression vectors: mRFP-Vps1-$FL_{1\text{-}704aa}$ (or mRFP-Vps1-Full length), mRFP-$Vps1_{1\text{-}340aa}$ (or mRFP-Vps1-GTPase), mRFP-$Vps1_{341\text{-}614aa}$ (or mRFP-Vps1-MID), mRFP-$Vps1_{615\text{-}704aa}$ (or mRFP-Vps1-GED), and mRFP-$Vps1_{341\text{-}704aa}$ (or mRFP-Vps1-

MID+GED) using KKD 0143 plasmid. After the introduction of mRFP-Vps1 or its domains into *vps1*Δ cells expressing Gga1-GFP, the extent of colocalization between them was determined. The Vps1 N-terminal 340aa was found to be completely cytoplasmic (Figure, 12, column 2), while full-length (column 1), the MID (column 3), the GED (column 4) and MID+GED domain (column 5) of Vps1 were partially targeted to the late Golgi marked by Gga1-GFP. Upon quantification, the full length Vps1 showed an average colocalization percentage of 25.4 % (± 4.0) with Gga1-GFP puncta, whereas, MID, GED, and MID+GED domains of Vps1 exhibited 13.55 % (± 3.2), 11.9 % (± 1.0), and 8.21% (± 3.21), respectively (Figure, 13). These results are suggestive that either the MID or GED domain of Vps1 is required for Vps1 targeting to the late Golgi.

DISCUSSION

Results from my study provide the first evidence for the direct interaction of Vps1 with clathrin, and thus provides an important insight into the potential mechanism of action of Vps1 in vesicular trafficking along with clathrin at the Golgi. Furthermore, my data provide evidence that Vps1 is implicated in the homeostasis of Golgi compartments, possibly mediating the fusion between late Golgi compartments. Finally, findings from my study offers invaluable insight into the Vps1 targeting mechanism to the Golgi.

Vps1 Functions with the Coat Protein Clathrin at the TGN

Research regarding CCV (clathrin-coated vesicle) formation at the Golgi in the budding yeast began in the early 1990s. It was suggested that Vps1 works in a coordinated manner with clathrin to facilitate the early event of vesicular trafficking occurring at the late Golgi (Conibear and Stevens, 1998). In particular, the investigators proposed that the dynamin-like protein Vps1 acts through its presumable intrinsic membrane pinching-off capacity. However, the coordinated action mechanism of Vps1 with clathrin (Chc1) at the Golgi is poorly understood. Consistent with this notion, it was reported that *VPS1* genetically interacts with *CHC1* and that a double mutant strain harboring a temperature sensitive allele of clathrin heavy chain (*chc1-521)* and a temperature sensitive allele of Vps1 (*vps1-ts*) exhibits more severe defects in the secretory traffic of α-factor than that of either single mutant (Bensen et al., 2000). These genetic interaction studies prompted me to investigate a hypothetical physical interaction of Vps1 with Chc1. Using the yeast two-hybrid system I discovered that the GTPase and

the GED domains, but not the MID, of Vps1 interact with the C-terminal domain of Chc1 that consists of 581 aa. Furthermore, in light of finding that the GTPase or the GED domain alone displayed stronger binding affinities to Chc1 than the full length of Vps1 did, one can conclude that each of these two domains contains its Chc1 binding site, and that the three dimensional association of these two domains in intact Vps1 may hinder, at least in part, the Chc1 binding patch of Vps1. Indeed, based on the crystal structure of mammalian dynamin, the GTPase and GED domains are closely situated (Faelber et al., 2012), and it is predicted that the two domains in Vps1 are positioned in close proximity to each other.

The C-terminal 581aa of Chc1 is predicted to carry a proximal and a trimerization domains, which are known to be involved in assembly and disassembly of the clathrin coat (Edeling et al., 2006). Interestingly, this C-terminal domain of Chc1 is reported to associate with clathrin binding proteins such as auxilin and Hsc70 proteins, which are implicated in clathrin uncoating or disassembly process (Fotin et al., 2004a, 2004b). Unlike these proteins, the vast majority of clathrin binding proteins, including endophilin and AP180, are known to interact with the N-terminal distal domain of clathrin, via the consensus clathrin binding motif sequence consisting of 6 amino acids, PLØPØP (where P is a polar amino acid, L is Leucine, and Ø is a hydrophobic amino acid) (Dell'Angelica et al., 1998). Notably, Vps1 contains the consensus sequence, $ELIDLN_{90\text{-}95aa}$ in its GTPase domain for the N-terminal region of Chc1. However, given the GTPase domain with the intact motif sequence does not bind to the N-terminal fragment of Chc1, it is concluded that the motif is non-functional for Chc1 binding.

The interaction of Vps1 to the C-terminal of Chc1 was unexpected and the significance of this type of binding is intriguing. Considering that the trimerization domain is implicated in forming a triskelion and the assembly of triskelions is necessary for the production of a clathrin cage, one can surmise that the direct interaction of Vps1 to the C-terminal Chc1 plays a role in clathrin recruitment and the subsequent assembly. In agreement with this idea, it was shown that recruitment of clathrin was blocked upon photoinactivation of dynamin in *D. melanogaster* (Kasprowicz et al., 2014). Consistently, my data showed that yeast clathrin targeting to the Golgi was severely disrupted in cells lacking Vps1, reminiscent of the abnormal phenotype found in *D. melanogaster.* If indeed Vps1 acts upstream of Chc1, it must be that Vps1 arrives at the Golgi before Chc1. The study of whether this is the case would require a sophisticated investigation into the spatiotemporal dynamics of Vps1 in relation with Chc1 at the Golgi. Upon recruitment, Vps1 may undergo self-assembly to form a ring of Vps1 polymer, as has been suggested by an in vitro experiment (Palmer et al., 2015). It may be that the Vps1 polymer then could serve as a scaffold for clathrin recruitment and assembly. It should be noted that mammalian dynamin binds to auxilin, a key player for clathrin uncoating (Newmyer et al., 2003), implying that dynamin could also serve as an upstream disassembly factor for clathrin. This raises the question of whether the recruitment of Swa2, the yeast homolog of mammalian auxilin (Troisi et al., 2015), to the clathrin cage depends on the presence of Vps1 in the budding yeast. Taken together, Vps1 appears to be intricately related to the regulation of clathrin assembly and disassembly dynamics at the Golgi.

Vps1 Targeting Mechanism to the TGN

Several lines of evidence revealed that dynamin and dynamin family proteins function at the Golgi membrane along with clathrin (Jones et al., 1998; Bonekamp et al., 2010). It has been proposed that dynamin's intrinsic membrane pinching-off activity is conserved at the Golgi, necessary for the formation of secretory vesicles (Cao et al., 2000; McNiven, 2000, 1998). To function at the Golgi, dynamin must to be first targeted to the corresponding site, for which it was thought that dynamin use its PH domain whose function is well known for mediating protein-phosphoinositide interactions (van der Bliek and Payne, 2010). Results from studies have revealed that few essential amino acid residues of the PH domain are implicated in the physical association of the PH domain with lipids. For example, the lysine 535 in the PH domain was proposed to directly interact with phosphoinositides (Achiriloaie et al., 1999). A recent study further revealed that dynamin mutant harboring a point mutation (I533A) in the β6/β7 loop of the PH domain abolished the recruitment or binding of the dynamin mutant to liposomes, indicating that the PH domain is required for dynamin targeting to the membrane (Bethoney et al., 2009). However, the same study showed that the mutations in PH domain did not affect the localization of dynamin to the plasma membrane in vivo, postulating a tentative role of the PRD domain of dynamin for its membrane targeting. In support of this view, McMahon's lab showed that full-length dynamin was only recruited to giant unilamellar vesicles (GUV) in the presence of endophilin that carries a SH3 domain, suggesting that the SH3 protein promotes more efficient recruitment of dynamin to membranes via an interaction with the PRD of dynamin (Meinecke et al., 2013).

Like the mammalian system, the budding yeast Vps1 recruitment to the endocytic site is dependent on a tentative PRD domain (or insert B) of Vps1, which interacts with the SH3 domain in the amphiphysin Rvs167 (Smaczynska-de Rooij et al., 2012). This result raises the question of whether Vps1 is targeted to the Golgi via it PRD domain interaction with Golgi-specific proteins, yet unidentified, carrying SH3 domain. Interestingly, the MID domain of Vps1, which carries a presumable proline rich motif (S-P-P-P-V, 598-602aa), was able to be targeted to the Golgi, albeit less efficiently compared with full length Vps1, pointing to the significance of protein-protein interaction for Vps1 targeting possibly via PRD-SH3 interaction between Vps1 and its binding partner at the Golgi. Yet, the direct evidence of Vps1 PRD recruitment toward the Golgi should be documented to prove the above-mentioned idea. Strikingly, my results showed that in addition to the MID domain, GED domain alone was associated with the Golgi. According to my sequence analysis, Vps1 does not contain the lipid binding consensus sequence, but near the C-terminal end is found several positively charged amino acids sequence (R-R-K-E-C-K-K, 683aa-689aa). Therefore, one possible explanation for the GED recruitment to the Golgi would be an electrostatic attraction between the GED and lipids on the Golgi membrane. The exact biochemical targeting of Vps1 to the Golgi should be further investigated in the near future.

Vps1 in the Shuttling Pathway Between the Golgi and the Endosome

Previously it was shown that loss of Vps1 led to the mistargeting of the alpha-factor receptor Kex2 and Vps10 to the late endosome and the vacuole (Chi et al., 2014; Nothwehr et al., 1995). In addition, Dr. Kim's lab recently found that Chc1 was

abnormally targeted to the late endosome and the vacuole in the same *vps1*Δ background strain (personal communication with our previous grad student, Michelle Williams). The molecular basis for the mistargeting of Kex2 to the endosomal compartment in cells deficient in Vps1 was proposed in 1995 by Nothwehr and coworkers (Nothwehr et al., 1995). The model suggests that loss of Vps1 results in a blockage in the anterograde traffic from the Golgi to the endosome, but does not affect the exocytic event. Under these conditions, Kex2 is first delivered to the plasma membrane and then destined for the endosomal system via endocytosis. The mistargeting of Vps10, the cargo receptor for carboxypeptidase (CPY), to the endosomal system can also be explained by the same model. Additionally, the Burd lab recently reported a severe accumulation of Vps10 at the endosome in cells lacking Vps1 and proposed a pinchase role of Vps1 for the exit of endosome-derived vesicles. What can be the possible explanation for clathrin mistargeting to the endosome, which I documented in the result section? Is there any connection between Vps10 accumulations with Chc1 mistargeting at the endosome in *vps1* mutant cells? An interesting clue to the understanding of this relationship was provided by data from a recent study that revealed that the recruitment of a subunit of AP2 (γ-adaptin) to the plasma membrane was disrupted in the cell where dynamin activity was abolished (Kasprowicz et al., 2014). From this finding, we can infer that loss of Vps1 may result in an aberrant targeting of the adaptor AP1 for Vps10 to the endosome due to accumulation of its cargo Vps10. If this scenario is the case, one can envision the subsequence recruitment of Chc1 to the endosome, since Chc1 has high binding affinity to AP1, but not to the cargo (Doray and Kornfeld, 2001). Even in the presence of the functional complex of cargo-adaptor-clathrin coat, the pinching-off of the

complex at the endosomal membrane appears to be inefficient due to lack of Vps1, a primary pinchase (Chi et al., 2014). Along with AP1, Gga1 , a well-known adaptor bridging cargo receptor to the clathrin (Ha et al., 2003), has been reported to function at the Golgi. However, Gga1-GFP was not mistargeted to the late endosome or vacuole in *vps1*Δ cells (Figure, 8), suggesting Vps1 acts specific for the targeting of Chc1 to the Golgi In other words, in the absence of Vps1 scaffold at the Golgi no clathrin is recruited, but Gga1's association with the Golgi is secured by an unknown reason. It is interesting to note that Sft2, a late Golgi marker whose precise function is unknown (Conchon et al., 1999), was mistargeted to the endosomal system. These results of mistargeting of only specific groups of proteins to the endosomal system suggest that loss of Vps1 does not globally affect the recruitment of Golgi proteins but rather its action is restricted to the selected group of proteins.

Increase in Number of Late Golgi in *vps1*Δ Cells

Rates of membrane fusion and fission regulate the overall size and the number of the Golgi (Bhave et al., 2014; Sengupta and Linstedt, 2011). Similarly, the copy number of a Golgi compartment could vary depending on certain parameters, such as rates of Golgi formation and its persistence time. The increase of the mean number of the late Golgi in *vps1* mutant cells (Figures, 10&11) suggests an aberrant Golgi homeostasis, possibly due to either homotypic Golgi fusion defects or alteration in Golgi persistence time, or due to both. To the best of my knowledge, the first direct evidence for homotypic fusion between late Golgi compartments derived from an *in vitro* vesicle fusion assay, which revealed that the yeast Rab5 homolog Vps21 and t-SNARE complex composed of Tlg1, Tlg2, Vti1 and v-SNARE Snc1 are required for late Golgi homotypic fusion

(Brickner et al., 2001). The notion that Vps1 might function for homotypic Golgi fusion is conceivable in fact because of few recent documents that support the role of dynamin and dynamin-like protein in membrane fusion. First, mammalian dynamin-2 binds to SNARE regulatory protein complexin 1 (Zhao et al., 2007) to modulate membrane fusion events during acrosomal exocytosis (Reid et al., 2012). Second, Peters' lab has shown that Vps1 binds to the Qa SNARE Vamp3 and controls trans-SNARE formation, which is essential for the homotypic vacuole fusion in yeast (Kulkarni et al., 2014). If indeed Vps1 entails the fusion between the late Golgi, it would be of great interest in understanding the functional relationship with Vps21 the upstream regulator for the homotypic fusion. Recently, Dr. Kim's lab discovered that Vps1 acting as an upstream regulator of the GARP tethering factor in the fusion of the endosome-derived vesicle with the Golgi (personal communication with our grad students). Given that the GARP factor works directly upstream of SNAREs, but downstream of Rab GTPase, I propose a series of interactions or signal transmission of Rab (Vps21)-Vps1-GARP-SNARE for homotypic Golgi fusion. Further studies are required to fully understand the functional niche of Vps1 in relation with the other important factors for homotypic Golgi fusion.

An alternative explanation for the increase in the number of late Golgi would be that the maturation time from early Golgi to the late Golgi is normal but the persistence time of late Golgi is longer in *vps1*Δ cells. This idea can be tested by using a simple quantitative framework P_E/P_L, where P_E is the average persistence time of early Golgi cisternae, and P_L is the average persistence time of late Golgi cisternae. The P_E/P_L ratio would be ~1 in wild-type cells (Bhave et al., 2014). Using Sed5, a fiduciary Cis-Golgi marker and GFP-PH FAPPI as a late Golgi marker, one can determine the average

persistence time of the late Golgi cisternae in WT and *vps1*Δ cells. If the ratio of P_E/P_L is <1.0 in *vps1*Δ cells, it can be concluded that the persistence time of the late Golgi is longer.

REFERENCES

Achiriloaie, M., Barylko, B., Albanesi, J.P., 1999. Essential role of the dynamin pleckstrin homology domain in receptor-mediated endocytosis. Mol. Cell. Biol. 19, 1410–5.

Almeida, C.G., Yamada, A., Tenza, D., Louvard, D., Raposo, G., Coudrier, E., 2011. Myosin 1b promotes the formation of post-Golgi carriers by regulating actin assembly and membrane remodelling at the trans-Golgi network. Nat. Cell Biol. 13, 779–89. doi:10.1038/ncb2262

Anitei, M., Hoflack, B., 2011a. Exit from the trans-Golgi network: from molecules to mechanisms. Curr. Opin. Cell Biol. 23, 443–51. doi:10.1016/j.ceb.2011.03.013

Anitei, M., Hoflack, B., 2011b. Bridging membrane and cytoskeleton dynamics in the secretory and endocytic pathways. Nat. Cell Biol. 14, 11–19. doi:10.1038/ncb2409

Anitei, M., Stange, C., Parshina, I., Baust, T., Schenck, A., Raposo, G., Kirchhausen, T., Hoflack, B., 2010a. Protein complexes containing CYFIP/Sra/PIR121 coordinate Arf1 and Rac1 signalling during clathrin-AP-1-coated carrier biogenesis at the TGN. Nat. Cell Biol. 12, 330–40. doi:10.1038/ncb2034

Anitei, M., Stange, C., Parshina, I., Baust, T., Schenck, A., Raposo, G., Kirchhausen, T., Hoflack, B., 2010b. Protein complexes containing CYFIP/Sra/PIR121 coordinate Arf1 and Rac1 signalling during clathrin-AP-1-coated carrier biogenesis at the TGN. Nat. Cell Biol. 12, 330–40. doi:10.1038/ncb2034

Anitei, M., Wassmer, T., Stange, C., Hoflack, B., 2010c. Bidirectional transport between the trans-Golgi network and the endosomal system. Mol. Membr. Biol. 27, 443–56. doi:10.3109/09687688.2010.522601

Audhya, A., Foti, M., Emr, S.D., 2000. Distinct roles for the yeast phosphatidylinositol 4-kinases, Stt4p and Pik1p, in secretion, cell growth, and organelle membrane dynamics. Mol. Biol. Cell 11, 2673–89.

Balderhaar, H.J. kleine, Ungermann, C., 2013. CORVET and HOPS tethering complexes - coordinators of endosome and lysosome fusion. J. Cell Sci. 126, 1307–16. doi:10.1242/jcs.107805

Bannykh, S.I., Balch, W.E., 1997. Membrane dynamics at the endoplasmic reticulum-Golgi interface. J. Cell Biol. 138, 1–4.

Becker, B., Melkonian, M., 1996. The secretory pathway of protists: spatial and functional organization and evolution. Microbiol. Rev. 60, 697–721.

Bensen, E.S., Costaguta, G., Payne, G.S., 2000. Synthetic genetic interactions with temperature-sensitive clathrin in Saccharomyces cerevisiae. Roles for synaptojanin-like Inp53p and dynamin-related Vps1p in clathrin-dependent protein sorting at the trans-Golgi network. Genetics 154, 83–97.

Bethoney, K.A., King, M.C., Hinshaw, J.E., Ostap, E.M., Lemmon, M.A., 2009. A possible effector role for the pleckstrin homology (PH) domain of dynamin. Proc. Natl. Acad. Sci. U. S. A. 106, 13359–64. doi:10.1073/pnas.0906945106

Bhave, M., Papanikou, E., Iyer, P., Pandya, K., Jain, B.K., Ganguly, A., Sharma, C., Pawar, K., Austin, J., Day, K.J., Rossanese, O.W., Glick, B.S., Bhattacharyya, D., 2014. Golgi enlargement in Arf-depleted yeast cells is due to altered dynamics of cisternal maturation. J. Cell Sci. 127, 250–7. doi:10.1242/jcs.140996

Bonekamp, N.A., Vormund, K., Jacob, R., Schrader, M., 2010. Dynamin-like protein 1 at the Golgi complex: a novel component of the sorting/targeting machinery en route to the plasma membrane. Exp. Cell Res. 316, 3454–67. doi:10.1016/j.yexcr.2010.07.020

Bonifacino, J.S., 2004. The GGA proteins: adaptors on the move. Nat. Rev. Mol. Cell Biol. 5, 23–32. doi:10.1038/nrm1279

Bonifacino, J.S., Glick, B.S., 2004. The mechanisms of vesicle budding and fusion. Cell 116, 153–66.

Bonifacino, J.S., Traub, L.M., 2003. Signals for sorting of transmembrane proteins to endosomes and lysosomes. Annu. Rev. Biochem. 72, 395–447. doi:10.1146/annurev.biochem.72.121801.161800

Bowers, K., Stevens, T.H., 2005. Protein transport from the late Golgi to the vacuole in the yeast Saccharomyces cerevisiae. Biochim. Biophys. Acta 1744, 438–54. doi:10.1016/j.bbamcr.2005.04.004

Brickner, J.H., Blanchette, J.M., Sipos, G., Fuller, R.S., 2001. The Tlg SNARE complex is required for TGN homotypic fusion. J. Cell Biol. 155, 969–78. doi:10.1083/jcb.200104093

Bröcker, C., Engelbrecht-Vandré, S., Ungermann, C., 2010. Multisubunit tethering complexes and their role in membrane fusion. Curr. Biol. 20, R943–52. doi:10.1016/j.cub.2010.09.015

Brown, F.C., Pfeffer, S.R., 2010. An update on transport vesicle tethering. Mol. Membr. Biol. 27, 457–61. doi:10.3109/09687688.2010.501765

Burd, C.G., Emr, S.D., 1998. Phosphatidylinositol(3)-phosphate signaling mediated by specific binding to RING FYVE domains. Mol. Cell 2, 157–62.

Burd, C.G., Peterson, M., Cowles, C.R., Emr, S.D., 1997. A novel Sec18p/NSF-dependent complex required for Golgi-to-endosome transport in yeast. Mol. Biol. Cell 8, 1089–104.

Cabrera, M., Arlt, H., Epp, N., Lachmann, J., Griffith, J., Perz, A., Reggiori, F., Ungermann, C., 2013. Functional separation of endosomal fusion factors and the class C core vacuole/endosome tethering (CORVET) complex in endosome biogenesis. J. Biol. Chem. 288, 5166–75. doi:10.1074/jbc.M112.431536

Cao, H., Thompson, H.M., Krueger, E.W., McNiven, M.A., 2000. Disruption of Golgi structure and function in mammalian cells expressing a mutant dynamin. J. Cell Sci. 113 Pt 1, 1993–2002

Chappie, J.S., Acharya, S., Leonard, M., Schmid, S.L., Dyda, F., 2010. G domain dimerization controls dynamin's assembly-stimulated GTPase activity. Nature 465, 435–40. doi:10.1038/nature09032

Chappie, J.S., Dyda, F., 2013. Building a fission machine--structural insights into dynamin assembly and activation. J. Cell Sci. 126, 2773–84. doi:10.1242/jcs.108845

Chappie, J.S., Mears, J.A., Fang, S., Leonard, M., Schmid, S.L., Milligan, R.A., Hinshaw, J.E., Dyda, F., 2011. A pseudoatomic model of the dynamin polymer identifies a hydrolysis-dependent powerstroke. Cell 147, 209–22. doi:10.1016/j.cell.2011.09.003

Chen, D.C., Yang, B.C., Kuo, T.T., 1992. One-step transformation of yeast in stationary phase. Curr. Genet. 21, 83–4.

Chi, R.J., Liu, J., West, M., Wang, J., Odorizzi, G., Burd, C.G., 2014. Fission of SNX-BAR-coated endosomal retrograde transport carriers is promoted by the dynamin-related protein Vps1. J. Cell Biol. 204, 793–806. doi:10.1083/jcb.201309084

Chirivino, D., Del Maestro, L., Formstecher, E., Hupé, P., Raposo, G., Louvard, D., Arpin, M., 2011. The ERM proteins interact with the HOPS complex to regulate the maturation of endosomes. Mol. Biol. Cell 22, 375–85. doi:10.1091/mbc.E10-09-0796

Cocucci, E., Gaudin, R., Kirchhausen, T., 2014. Dynamin recruitment and membrane scission at the neck of a clathrin-coated pit. Mol. Biol. Cell 25, 3595–609. doi:10.1091/mbc.E14-07-1240

Conchon, S., Cao, X., Barlowe, C., Pelham, H.R., 1999. Got1p and Sft2p: membrane proteins involved in traffic to the Golgi complex. EMBO J. 18, 3934–46. doi:10.1093/emboj/18.14.3934

Conibear, E., Stevens, T.H., 1995. Vacuolar biogenesis in yeast: Sorting out the sorting proteins. Cell 83, 513–516. doi:10.1016/0092-8674(95)90088-8

Conibear, E., Stevens, T.H., 1998. Multiple sorting pathways between the late Golgi and the vacuole in yeast. Biochim. Biophys. Acta 1404, 211–30.

Cooper, A.A., Stevens, T.H., 1996. Vps10p cycles between the late-Golgi and prevacuolar compartments in its function as the sorting receptor for multiple yeast vacuolar hydrolases. J. Cell Biol. 133, 529–41.

Coudrier, E., Almeida, C.G., 2011. Myosin 1 controls membrane shape by coupling F-Actin to membrane. Bioarchitecture 1, 230–235. doi:10.4161/bioa.18406

Cowles, C.R., Odorizzi, G., Payne, G.S., Emr, S.D., 1997. The AP-3 adaptor complex is essential for cargo-selective transport to the yeast vacuole. Cell 91, 109–18.

D'Souza-Schorey, C., Chavrier, P., 2006. ARF proteins: roles in membrane traffic and beyond. Nat. Rev. Mol. Cell Biol. 7, 347–58. doi:10.1038/nrm1910

Daboussi, L., Costaguta, G., Payne, G.S., 2012. Phosphoinositide-mediated clathrin adaptor progression at the trans-Golgi network. Nat. Cell Biol. 14, 239–48. doi:10.1038/ncb2427

Dacks, J.B., Davis, L.A.M., Sjögren, A.M., Andersson, J.O., Roger, A.J., Doolittle, W.F., 2003. Evidence for Golgi bodies in proposed "Golgi-lacking" lineages. Proc. Biol. Sci. 270 Suppl , S168–71. doi:10.1098/rsbl.2003.0058

Day, K.J., Staehelin, L.A., Glick, B.S., 2013. A three-stage model of Golgi structure and function. Histochem. Cell Biol. 140, 239–49. doi:10.1007/s00418-013-1128-3

De Matteis, M.A., Luini, A., 2008. Exiting the Golgi complex. Nat. Rev. Mol. Cell Biol. 9, 273–84. doi:10.1038/nrm2378

Delevoye, C., Hurbain, I., Tenza, D., Sibarita, J.-B., Uzan-Gafsou, S., Ohno, H., Geerts, W.J.C., Verkleij, A.J., Salamero, J., Marks, M.S., Raposo, G., 2009. AP-1 and KIF13A coordinate endosomal sorting and positioning during melanosome biogenesis. J. Cell Biol. 187, 247–64. doi:10.1083/jcb.200907122

Dell'Angelica, E.C., Klumperman, J., Stoorvogel, W., Bonifacino, J.S., 1998. Association of the AP-3 adaptor complex with clathrin. Science 280, 431–4.

Dilcher, M., Köhler, B., von Mollard, G.F., 2001. Genetic interactions with the yeast Q-SNARE VTI1 reveal novel functions for the R-SNARE YKT6. J. Biol. Chem. 276, 34537–44. doi:10.1074/jbc.M101551200

Dippold, H.C., Ng, M.M., Farber-Katz, S.E., Lee, S.-K., Kerr, M.L., Peterman, M.C., Sim, R., Wiharto, P.A., Galbraith, K.A., Madhavarapu, S., Fuchs, G.J., Meerloo, T., Farquhar, M.G., Zhou, H., Field, S.J., 2009. GOLPH3 bridges phosphatidylinositol-4- phosphate and actomyosin to stretch and shape the Golgi to promote budding. Cell 139, 337–51. doi:10.1016/j.cell.2009.07.052

Domozych, D.S., 1991. The Golgi apparatus and membrane trafficking in green algae. Int. Rev. Cytol. 131, 213–53.

Donaldson, J.G., Honda, A., Weigert, R., 2005. Multiple activities for Arf1 at the Golgi complex. Biochim. Biophys. Acta 1744, 364–73. doi:10.1016/j.bbamcr.2005.03.001

Doray, B., Kornfeld, S., 2001. Gamma subunit of the AP-1 adaptor complex binds clathrin: implications for cooperative binding in coated vesicle assembly. Mol. Biol. Cell 12, 1925–35.

Dowler, S., Currie, R.A., Campbell, D.G., Deak, M., Kular, G., Downes, C.P., Alessi, D.R., 2000. Identification of pleckstrin-homology-domain-containing proteins with novel phosphoinositide-binding specificities. Biochem. J. 351, 19–31.

Duncan, M.C., Payne, G.S., 2003. ENTH/ANTH domains expand to the Golgi. Trends Cell Biol. 13, 211–5.

Edeling, M.A., Smith, C., Owen, D., 2006. Life of a clathrin coat: insights from clathrin and AP structures. Nat. Rev. Mol. Cell Biol. 7, 32–44. doi:10.1038/nrm1786

Faelber, K., Held, M., Gao, S., Posor, Y., Haucke, V., Noé, F., Daumke, O., 2012. Structural insights into dynamin-mediated membrane fission. Structure 20, 1621–8. doi:10.1016/j.str.2012.08.028

Farquhar, M.G., Palade, G.E., 1981. The Golgi apparatus (complex)-(1954-1981)-from artifact to center stage. J. Cell Biol. 91, 77s–103s.

Fasshauer, D., Sutton, R.B., Brunger, A.T., Jahn, R., 1998. Conserved structural features of the synaptic fusion complex: SNARE proteins reclassified as Q- and R-SNAREs. Proc. Natl. Acad. Sci. U. S. A. 95, 15781–6.

Ferguson, S.M., Ferguson, S., Raimondi, A., Paradise, S., Shen, H., Mesaki, K., Ferguson, A., Destaing, O., Ko, G., Takasaki, J., Cremona, O., O' Toole, E., De Camilli, P., 2009. Coordinated actions of actin and BAR proteins upstream of dynamin at endocytic clathrin-coated pits. Dev. Cell 17, 811–22. doi:10.1016/j.devcel.2009.11.005

Fölsch, H., Ohno, H., Bonifacino, J.S., Mellman, I., 1999. A novel clathrin adaptor complex mediates basolateral targeting in polarized epithelial cells. Cell 99, 189–98.

Fotin, A., Cheng, Y., Grigorieff, N., Walz, T., Harrison, S.C., Kirchhausen, T., 2004a. Structure of an auxilin-bound clathrin coat and its implications for the mechanism of uncoating. Nature 432, 649–53. doi:10.1038/nature03078

Fotin, A., Cheng, Y., Sliz, P., Grigorieff, N., Harrison, S.C., Kirchhausen, T., Walz, T., 2004b. Molecular model for a complete clathrin lattice from electron cryomicroscopy. Nature 432, 573–9. doi:10.1038/nature03079

Frost, A., Unger, V.M., Camilli, P. De, 2000. Boomerangs, Bananas and Blimps: Structure and Function of F-BAR Domains in the Context of the BAR Domain Superfamily.

Furukawa, N., Mima, J., 2014. Multiple and distinct strategies of yeast SNAREs to confer the specificity of membrane fusion. Sci. Rep. 4, 4277. doi:10.1038/srep04277

Gao, S., von der Malsburg, A., Paeschke, S., Behlke, J., Haller, O., Kochs, G., Daumke, O., 2010. Structural basis of oligomerization in the stalk region of dynamin-like MxA. Nature 465, 502–6. doi:10.1038/nature08972

Gehart, H., Goginashvili, A., Beck, R., Morvan, J., Erbs, E., Formentini, I., De Matteis, M.A., Schwab, Y., Wieland, F.T., Ricci, R., 2012. The BAR domain protein Arfaptin-1 controls secretory granule biogenesis at the trans-Golgi network. Dev. Cell 23, 756–68. doi:10.1016/j.devcel.2012.07.019

Ghosh, P., Dahms, N.M., Kornfeld, S., 2003. Mannose 6-phosphate receptors: new twists in the tale. Nat. Rev. Mol. Cell Biol. 4, 202–12. doi:10.1038/nrm1050

Gillooly, D.J., Morrow, I.C., Lindsay, M., Gould, R., Bryant, N.J., Gaullier, J.M., Parton, R.G., Stenmark, H., 2000. Localization of phosphatidylinositol 3-phosphate in yeast and mammalian cells. EMBO J. 19, 4577–88. doi:10.1093/emboj/19.17.4577

Glick, B.S., Nakano, A., 2009. Membrane traffic within the Golgi apparatus. Annu. Rev. Cell Dev. Biol. 25, 113–32. doi:10.1146/annurev.cellbio.24.110707.175421

Grassart, A., Cheng, A.T., Hong, S.H., Zhang, F., Zenzer, N., Feng, Y., Briner, D.M., Davis, G.D., Malkov, D., Drubin, D.G., 2014. Actin and dynamin2 dynamics and interplay during clathrin-mediated endocytosis. J. Cell Biol. 205, 721–35. doi:10.1083/jcb.201403041

Ha, S.-A., Torabinejad, J., DeWald, D.B., Wenk, M.R., Lucast, L., De Camilli, P., Newitt, R.A., Aebersold, R., Nothwehr, S.F., 2003. The synaptojanin-like protein Inp53/Sjl3 functions with clathrin in a yeast TGN-to-endosome pathway distinct

from the GGA protein-dependent pathway. Mol. Biol. Cell 14, 1319–33. doi:10.1091/mbc.E02-10-0686

Hammond, A.T., Glick, B.S., 2000. Dynamics of transitional endoplasmic reticulum sites in vertebrate cells. Mol. Biol. Cell 11, 3013–30.

Hayden, J., Williams, M., Granich, A., Ahn, H., Tenay, B., Lukehart, J., Highfill, C., Dobard, S., Kim, K., 2013. Vps1 in the late endosome-to-vacuole traffic. J. Biosci. 38, 73–83.

Hirokawa, N., Noda, Y., Tanaka, Y., Niwa, S., 2009. Kinesin superfamily motor proteins and intracellular transport. Nat. Rev. Mol. Cell Biol. 10, 682–96. doi:10.1038/nrm2774

Hong, W., 2005. SNAREs and traffic. Biochim. Biophys. Acta 1744, 120–44. doi:10.1016/j.bbamcr.2005.03.014

Hong, W., Lev, S., 2014. Tethering the assembly of SNARE complexes. Trends Cell Biol. 24, 35–43. doi:10.1016/j.tcb.2013.09.006

Horiuchi, H., Lippé, R., McBride, H.M., Rubino, M., Woodman, P., Stenmark, H., Rybin, V., Wilm, M., Ashman, K., Mann, M., Zerial, M., 1997. A novel Rab5 GDP/GTP exchange factor complexed to Rabaptin-5 links nucleotide exchange to effector recruitment and function. Cell 90, 1149–59.

Howell, G.J., Holloway, Z.G., Cobbold, C., Monaco, A.P., Ponnambalam, S., 2006. Cell biology of membrane trafficking in human disease. Int. Rev. Cytol. 252, 1–69. doi:10.1016/S0074-7696(06)52005-4

Jahn, R., Scheller, R.H., 2006. SNAREs--engines for membrane fusion. Nat. Rev. Mol. Cell Biol. 7, 631–43. doi:10.1038/nrm2002

Jones, S.M., Howell, K.E., Henley, J.R., Cao, H., McNiven, M.A., 1998. Role of dynamin in the formation of transport vesicles from the trans-Golgi network. Science 279, 573–7.

Kang, B.-H., Nielsen, E., Preuss, M.L., Mastronarde, D., Staehelin, L.A., 2011. Electron tomography of RabA4b- and PI-4Kβ1-labeled trans Golgi network compartments in Arabidopsis. Traffic 12, 313–29. doi:10.1111/j.1600-0854.2010.01146.x

Kasprowicz, J., Kuenen, S., Swerts, J., Miskiewicz, K., Verstreken, P., 2014. Dynamin photoinactivation blocks Clathrin and α-adaptin recruitment and induces bulk membrane retrieval. J. Cell Biol. 204, 1141–56. doi:10.1083/jcb.201310090

Kim, K., Galletta, B.J., Schmidt, K.O., Chang, F.S., Blumer, K.J., Cooper, J.A., 2006. Actin-based motility during endocytosis in budding yeast. Mol. Biol. Cell 17, 1354–63. doi:10.1091/mbc.E05-10-0925

Klumperman, J., 2011. Architecture of the mammalian Golgi. Cold Spring Harb. Perspect. Biol. 3. doi:10.1101/cshperspect.a005181

Kornfeld, S., 1992. Structure and function of the mannose 6-phosphate/insulinlike growth factor II receptors. Annu. Rev. Biochem. 61, 307–30. doi:10.1146/annurev.bi.61.070192.001515

Koster, G., VanDuijn, M., Hofs, B., Dogterom, M., 2003. Membrane tube formation from giant vesicles by dynamic association of motor proteins. Proc. Natl. Acad. Sci. U. S. A. 100, 15583–8. doi:10.1073/pnas.2531786100

Kreitzer, G., Marmorstein, A., Okamoto, P., Vallee, R., Rodriguez-Boulan, E., 2000. Kinesin and dynamin are required for post-Golgi transport of a plasma-membrane protein. Nat. Cell Biol. 2, 125–7. doi:10.1038/35000081

Kulkarni, A., Alpadi, K., Sirupangi, T., Peters, C., 2014. A dynamin homolog promotes the transition from hemifusion to content mixing in intracellular membrane fusion. Traffic 15, 558–71. doi:10.1111/tra.12156

Kümmel, D., Ungermann, C., 2014. Principles of membrane tethering and fusion in endosome and lysosome biogenesis. Curr. Opin. Cell Biol. 29, 61–6. doi:10.1016/j.ceb.2014.04.007

Kweon, Y., Rothe, A., Conibear, E., Stevens, T.H., 2003. Ykt6p is a multifunctional yeast R-SNARE that is required for multiple membrane transport pathways to the vacuole. Mol. Biol. Cell 14, 1868–81. doi:10.1091/mbc.E02-10-0687

Lewis, M.J., Pelham, H.R.B., 2002. A new yeast endosomal SNARE related to mammalian syntaxin 8. Traffic 3, 922–9.

Longtine, M.S., Mckenzie III, A., Demarini, D.J., Shah, N.G., Wach, A., Brachat, A., Philippsen, P., Pringle, J.R., 1998. Additional modules for versatile and economical PCR-based gene deletion and modification in Saccharomyces cerevisiae. Yeast 14, 953–961. doi:10.1002/(SICI)1097-0061(199807)14:10<953::AID-YEA293>3.0.CO;2-U

Lukehart, J., Highfill, C., Kim, K., 2013. Vps1, a recycling factor for the traffic from early endosome to the late Golgi. Biochem. Cell Biol. 91, 455–65. doi:10.1139/bcb-2013-0044

Malsam, J., Söllner, T.H., 2011. Organization of SNAREs within the Golgi stack. Cold Spring Harb. Perspect. Biol. 3, a005249. doi:10.1101/cshperspect.a005249

Marcusson, E.G., Horazdovsky, B.F., Cereghino, J.L., Gharakhanian, E., Emr, S.D., 1994. The sorting receptor for yeast vacuolar carboxypeptidase Y is encoded by the VPS10 gene. Cell 77, 579–86.

Markgraf, D.F., Ahnert, F., Arlt, H., Mari, M., Peplowska, K., Epp, N., Griffith, J., Reggiori, F., Ungermann, C., 2009. The CORVET subunit Vps8 cooperates with the Rab5 homolog Vps21 to induce clustering of late endosomal compartments. Mol. Biol. Cell 20, 5276–89. doi:10.1091/mbc.E09-06-0521

Mayer, A., Wickner, W., Haas, A., 1996. Sec18p (NSF)-driven release of Sec17p (alpha-SNAP) can precede docking and fusion of yeast vacuoles. Cell 85, 83–94.

McMahon, H.T., Gallop, J.L., 2005. Membrane curvature and mechanisms of dynamic cell membrane remodelling. Nature 438, 590–6. doi:10.1038/nature04396

McNiven, M., 2000. The dynamin family of mechanoenzymes: pinching in new places. Trends Biochem. Sci. 25, 115–120. doi:10.1016/S0968-0004(99)01538-8

McNiven, M.A., 1998. Dynamin: a molecular motor with pinchase action. Cell 94, 151–4.

McNiven, M.A., Thompson, H.M., 2006. Vesicle formation at the plasma membrane and trans-Golgi network: the same but different. Science 313, 1591–4. doi:10.1126/science.1118133

Mears, J.A., Lackner, L.L., Fang, S., Ingerman, E., Nunnari, J., Hinshaw, J.E., 2011. Conformational changes in Dnm1 support a contractile mechanism for mitochondrial fission. Nat. Struct. Mol. Biol. 18, 20–6. doi:10.1038/nsmb.1949

Meinecke, M., Boucrot, E., Camdere, G., Hon, W.-C., Mittal, R., McMahon, H.T., 2013. Cooperative recruitment of dynamin and BIN/amphiphysin/Rvs (BAR) domain-containing proteins leads to GTP-dependent membrane scission. J. Biol. Chem. 288, 6651–61. doi:10.1074/jbc.M112.444869

Mellman, I., Simons, K., 1992. The Golgi complex: in vitro veritas? Cell 68, 829–40.

Mettlen, M., Pucadyil, T., Ramachandran, R., Schmid, S.L., 2009. Dissecting dynamin's role in clathrin-mediated endocytosis. Biochem. Soc. Trans. 37, 1022–6. doi:10.1042/BST0371022

Mishra, A., Eathiraj, S., Corvera, S., Lambright, D.G., 2010. Structural basis for Rab GTPase recognition and endosome tethering by the C2H2 zinc finger of Early Endosomal Autoantigen 1 (EEA1). Proc. Natl. Acad. Sci. U. S. A. 107, 10866–71. doi:10.1073/pnas.1000843107

Mogelsvang, S., Gomez-Ospina, N., Soderholm, J., Glick, B.S., Staehelin, L.A., 2003. Tomographic evidence for continuous turnover of Golgi cisternae in Pichia pastoris. Mol. Biol. Cell 14, 2277–91. doi:10.1091/mbc.E02-10-0697

Morrison, H.A., Dionne, H., Rusten, T.E., Brech, A., Fisher, W.W., Pfeiffer, B.D., Celniker, S.E., Stenmark, H., Bilder, D., 2008. Regulation of early endosomal entry by the Drosophila tumor suppressors Rabenosyn and Vps45. Mol. Biol. Cell 19, 4167–76. doi:10.1091/mbc.E08-07-0716

Nakagawa, T., Setou, M., Seog, D., Ogasawara, K., Dohmae, N., Takio, K., Hirokawa, N., 2000. A novel motor, KIF13A, transports mannose-6-phosphate receptor to plasma membrane through direct interaction with AP-1 complex. Cell 103, 569–81.

Nannapaneni, S., Wang, D., Jain, S., Schroeder, B., Highfill, C., Reustle, L., Pittsley, D., Maysent, A., Moulder, S., McDowell, R., Kim, K., 2010. The yeast dynamin-like protein Vps1:vps1 mutations perturb the internalization and the motility of endocytic vesicles and endosomes via disorganization of the actin cytoskeleton. Eur. J. Cell Biol. 89, 499–508. doi:10.1016/j.ejcb.2010.02.002

Newmyer, S.L., Christensen, A., Sever, S., 2003. Auxilin-dynamin interactions link the uncoating ATPase chaperone machinery with vesicle formation. Dev. Cell 4, 929–40.

Nothwehr, S.F., Conibear, E., Stevens, T.H., 1995. Golgi and vacuolar membrane proteins reach the vacuole in vps1 mutant yeast cells via the plasma membrane. J. Cell Biol. 129, 35–46.

Obara, K., Kojima, R., Kihara, A., 2013. Effects on vesicular transport pathways at the late endosome in cells with limited very long-chain fatty acids. J. Lipid Res. 54, 831–42. doi:10.1194/jlr.M034678

Odorizzi, G., Babst, M., Emr, S.D., 1998. Fab1p PtdIns(3)P 5-Kinase Function Essential for Protein Sorting in the Multivesicular Body. Cell 95, 847–858. doi:10.1016/S0092-8674(00)81707-9

Ohya, T., Miaczynska, M., Coskun, U., Lommer, B., Runge, A., Drechsel, D., Kalaidzidis, Y., Zerial, M., 2009. Reconstitution of Rab- and SNARE-dependent membrane fusion by synthetic endosomes. Nature 459, 1091–7. doi:10.1038/nature08107

Ostrowicz, C.W., Bröcker, C., Ahnert, F., Nordmann, M., Lachmann, J., Peplowska, K., Perz, A., Auffarth, K., Engelbrecht-Vandré, S., Ungermann, C., 2010. Defined subunit arrangement and rab interactions are required for functionality of the HOPS tethering complex. Traffic 11, 1334–46. doi:10.1111/j.1600-0854.2010.01097.x

Palmer, S.E., Smaczynska-de Rooij, I.I., Marklew, C.J., Allwood, E.G., Mishra, R., Johnson, S., Goldberg, M.W., Ayscough, K.R., 2015. A dynamin-actin interaction is required for vesicle scission during endocytosis in yeast. Curr. Biol. 25, 868–78. doi:10.1016/j.cub.2015.01.061

Papanikou, E., Glick, B.S., 2009. The yeast Golgi apparatus: insights and mysteries. FEBS Lett. 583, 3746–51. doi:10.1016/j.febslet.2009.10.072

Papanikou, E., Glick, B.S., 2014. Golgi compartmentation and identity. Curr. Opin. Cell Biol. 29, 74–81. doi:10.1016/j.ceb.2014.04.010

Parlati, F., Varlamov, O., Paz, K., McNew, J.A., Hurtado, D., Söllner, T.H., Rothman, J.E., 2002. Distinct SNARE complexes mediating membrane fusion in Golgi transport based on combinatorial specificity. Proc. Natl. Acad. Sci. U. S. A. 99, 5424–9. doi:10.1073/pnas.082100899

Peplowska, K., Markgraf, D.F., Ostrowicz, C.W., Bange, G., Ungermann, C., 2007. The CORVET tethering complex interacts with the yeast Rab5 homolog Vps21 and is involved in endo-lysosomal biogenesis. Dev. Cell 12, 739–50. doi:10.1016/j.devcel.2007.03.006

Peter, B.J., Kent, H.M., Mills, I.G., Vallis, Y., Butler, P.J.G., Evans, P.R., McMahon, H.T., 2004. BAR domains as sensors of membrane curvature: the amphiphysin BAR structure. Science 303, 495–9. doi:10.1126/science.1092586

Peterson, M.R., Emr, S.D., 2001. The class C Vps complex functions at multiple stages of the vacuolar transport pathway. Traffic 2, 476–86.

Pobbati, A. V, Stein, A., Fasshauer, D., 2006. N- to C-terminal SNARE complex assembly promotes rapid membrane fusion. Science 313, 673–6. doi:10.1126/science.1129486

Polishchuk, E. V, Di Pentima, A., Luini, A., Polishchuk, R.S., 2003. Mechanism of constitutive export from the golgi: bulk flow via the formation, protrusion, and en bloc cleavage of large trans-golgi network tubular domains. Mol. Biol. Cell 14, 4470–85. doi:10.1091/mbc.E03-01-0033

Praefcke, G.J.K., McMahon, H.T., 2004. The dynamin superfamily: universal membrane tubulation and fission molecules? Nat. Rev. Mol. Cell Biol. 5, 133–47. doi:10.1038/nrm1313

Prydz, K., Dick, G., Tveit, H., 2008. How many ways through the Golgi maze? Traffic 9, 299–304. doi:10.1111/j.1600-0854.2007.00690.x

Pryor, P.R., Mullock, B.M., Bright, N.A., Lindsay, M.R., Gray, S.R., Richardson, S.C.W., Stewart, A., James, D.E., Piper, R.C., Luzio, J.P., 2004. Combinatorial

SNARE complexes with VAMP7 or VAMP8 define different late endocytic fusion events. EMBO Rep. 5, 590–5. doi:10.1038/sj.embor.7400150

Puertollano, R., 2004. Clathrin-mediated transport: assembly required. Workshop on Molecular Mechanisms of Vesicle Selectivity. EMBO Rep. 5, 942–6. doi:10.1038/sj.embor.7400249

Puertollano, R., Bonifacino, J.S., 2004. Interactions of GGA3 with the ubiquitin sorting machinery. Nat. Cell Biol. 6, 244–51. doi:10.1038/ncb1106

Puertollano, R., Randazzo, P.A., Presley, J.F., Hartnell, L.M., Bonifacino, J.S., 2001. The GGAs promote ARF-dependent recruitment of clathrin to the TGN. Cell 105, 93–102.

Rabouille, C., Kondylis, V., 2007. Golgi ribbon unlinking: an organelle-based G2/M checkpoint. Cell Cycle 6, 2723–9.

Ramachandran, R., 2011. Vesicle scission: dynamin. Semin. Cell Dev. Biol. 22, 10–7. doi:10.1016/j.semcdb.2010.09.001

Reid, A.T., Lord, T., Stanger, S.J., Roman, S.D., McCluskey, A., Robinson, P.J., Aitken, R.J., Nixon, B., 2012. Dynamin regulates specific membrane fusion events necessary for acrosomal exocytosis in mouse spermatozoa. J. Biol. Chem. 287, 37659–72. doi:10.1074/jbc.M112.392803

Robinson, M.S., 2004. Adaptable adaptors for coated vesicles. Trends Cell Biol. 14, 167–74. doi:10.1016/j.tcb.2004.02.002

Rottner, K., Hänisch, J., Campellone, K.G., 2010. WASH, WHAMM and JMY: regulation of Arp2/3 complex and beyond. Trends Cell Biol. 20, 650–61. doi:10.1016/j.tcb.2010.08.014

Roux, A., Cappello, G., Cartaud, J., Prost, J., Goud, B., Bassereau, P., 2002. A minimal system allowing tubulation with molecular motors pulling on giant liposomes. Proc. Natl. Acad. Sci. U. S. A. 99, 5394–9. doi:10.1073/pnas.082107299

Santiago-Tirado, F.H., Bretscher, A., 2011. Membrane-trafficking sorting hubs: cooperation between PI4P and small GTPases at the trans-Golgi network. Trends Cell Biol. 21, 515–25. doi:10.1016/j.tcb.2011.05.005

Schmid, S.L., Frolov, V.A., 2011. Dynamin: functional design of a membrane fission catalyst. Annu. Rev. Cell Dev. Biol. 27, 79–105. doi:10.1146/annurev-cellbio-100109-104016

Schmidt, M.R., Maritzen, T., Kukhtina, V., Higman, V.A., Doglio, L., Barak, N.N., Strauss, H., Oschkinat, H., Dotti, C.G., Haucke, V., 2009. Regulation of endosomal

membrane traffic by a Gadkin/AP-1/kinesin KIF5 complex. Proc. Natl. Acad. Sci. U. S. A. 106, 15344–9. doi:10.1073/pnas.0904268106

Scott, P.M., Bilodeau, P.S., Zhdankina, O., Winistorfer, S.C., Hauglund, M.J., Allaman, M.M., Kearney, W.R., Robertson, A.D., Boman, A.L., Piper, R.C., 2004. GGA proteins bind ubiquitin to facilitate sorting at the trans-Golgi network. Nat. Cell Biol. 6, 252–9. doi:10.1038/ncb1107

Seaman, M.N.J., 1997. Endosome to Golgi Retrieval of the Vacuolar Protein Sorting Receptor, Vps10p, Requires the Function of the VPS29, VPS30, and VPS35 Gene Products. J. Cell Biol. 137, 79–92. doi:10.1083/jcb.137.1.79

Seaman, M.N.J., Gautreau, A., Billadeau, D.D., 2013. Retromer-mediated endosomal protein sorting: all WASHed up! Trends Cell Biol. 23, 522–8. doi:10.1016/j.tcb.2013.04.010

Sengupta, D., Linstedt, A.D., 2011. Control of organelle size: the Golgi complex. Annu. Rev. Cell Dev. Biol. 27, 57–77. doi:10.1146/annurev-cellbio-100109-104003

Smaczynska-de Rooij, I.I., Allwood, E.G., Mishra, R., Booth, W.I., Aghamohammadzadeh, S., Goldberg, M.W., Ayscough, K.R., 2012. Yeast dynamin Vps1 and amphiphysin Rvs167 function together during endocytosis. Traffic 13, 317–28. doi:10.1111/j.1600-0854.2011.01311.x

Sriram, V., Krishnan, K.S., Mayor, S., 2003. deep-orange and carnation define distinct stages in late endosomal biogenesis in Drosophila melanogaster. J. Cell Biol. 161, 593–607. doi:10.1083/jcb.200210166

Stefan, C.J., Audhya, A., Emr, S.D., 2002. The yeast synaptojanin-like proteins control the cellular distribution of phosphatidylinositol (4,5)-bisphosphate. Mol. Biol. Cell 13, 542–57. doi:10.1091/mbc.01-10-0476

Stenmark, H., 2009. Rab GTPases as coordinators of vesicle traffic. Nat. Rev. Mol. Cell Biol. 10, 513–25. doi:10.1038/nrm2728

Strahl, T., Hama, H., DeWald, D.B., Thorner, J., 2005. Yeast phosphatidylinositol 4-kinase, Pik1, has essential roles at the Golgi and in the nucleus. J. Cell Biol. 171, 967–79. doi:10.1083/jcb.200504104

Suarez, A., Ueno, T., Huebner, R., McCaffery, J.M., Inoue, T., 2014. Bin/Amphiphysin/Rvs (BAR) family members bend membranes in cells. Sci. Rep. 4, 4693. doi:10.1038/srep04693

Subramanian, S., Woolford, C.A., Jones, E.W., 2004. The Sec1/Munc18 protein, Vps33p, functions at the endosome and the vacuole of Saccharomyces cerevisiae. Mol. Biol. Cell 15, 2593–605. doi:10.1091/mbc.E03-10-0767

Suda, Y., Nakano, A., 2012. The yeast Golgi apparatus. Traffic 13, 505–10. doi:10.1111/j.1600-0854.2011.01316.x

Suetsugu, S., 2009. The direction of actin polymerization for vesicle fission suggested from membranes tubulated by the EFC/F-BAR domain protein FBP17. FEBS Lett. 583, 3401–4. doi:10.1016/j.febslet.2009.10.019

Szul, T., Sztul, E., 2011. COPII and COPI traffic at the ER-Golgi interface. Physiology (Bethesda). 26, 348–64. doi:10.1152/physiol.00017.2011

Taylor, M.J., Lampe, M., Merrifield, C.J., 2012. A feedback loop between dynamin and actin recruitment during clathrin-mediated endocytosis. PLoS Biol. 10, e1001302. doi:10.1371/journal.pbio.1001302

Theos, A.C., Tenza, D., Martina, J.A., Hurbain, I., Peden, A.A., Sviderskaya, E. V, Stewart, A., Robinson, M.S., Bennett, D.C., Cutler, D.F., Bonifacino, J.S., Marks, M.S., Raposo, G., 2005. Functions of adaptor protein (AP)-3 and AP-1 in tyrosinase sorting from endosomes to melanosomes. Mol. Biol. Cell 16, 5356–72. doi:10.1091/mbc.E05-07-0626

Thyberg, J., Moskalewski, S., 1985. Microtubules and the organization of the Golgi complex. Exp. Cell Res. 159, 1–16.

Thyberg, J., Moskalewski, S., 1999. Role of microtubules in the organization of the Golgi complex. Exp. Cell Res. 246, 263–79. doi:10.1006/excr.1998.4326

Troisi, E.M., Rockman, M.E., Nguyen, P.P., Oliver, E.E., Hines, J.K., 2015. Swa2, the yeast homolog of mammalian auxilin, is specifically required for the propagation of the prion variant [URE3-1]. Mol. Microbiol. 97, 926–41. doi:10.1111/mmi.13076

Van der Bliek, A.M., Payne, G.S., 2010. Dynamin subunit interactions revealed. Dev. Cell 18, 687–8. doi:10.1016/j.devcel.2010.05.001

Vicinanza, M., D'Angelo, G., Di Campli, A., De Matteis, M.A., 2008. Function and dysfunction of the PI system in membrane trafficking. EMBO J. 27, 2457–70. doi:10.1038/emboj.2008.169

Wang, Y.J., Wang, J., Sun, H.Q., Martinez, M., Sun, Y.X., Macia, E., Kirchhausen, T., Albanesi, J.P., Roth, M.G., Yin, H.L., 2003. Phosphatidylinositol 4 phosphate regulates targeting of clathrin adaptor AP-1 complexes to the Golgi. Cell 114, 299–310.

Webb, G.C., Zhang, J., Garlow, S.J., Wesp, A., Riezman, H., Jones, E.W., 1997. Pep7p provides a novel protein that functions in vesicle-mediated transport between the yeast Golgi and endosome. Mol. Biol. Cell 8, 871–95.

Wei, J.-H., Seemann, J., 2010. Unraveling the Golgi ribbon. Traffic 11, 1391–400. doi:10.1111/j.1600-0854.2010.01114.x

Weisz, O.A., Rodriguez-Boulan, E., 2009. Apical trafficking in epithelial cells: signals, clusters and motors. J. Cell Sci. 122, 4253–66. doi:10.1242/jcs.032615

Whiteheart, S.W., Griff, I.C., Brunner, M., Clary, D.O., Mayer, T., Buhrow, S.A., Rothman, J.E., 1993. SNAP family of NSF attachment proteins includes a brain-specific isoform. Nature 362, 353–5. doi:10.1038/362353a0

Wiedemann, C., Schäfer, T., Burger, M.M., 1996. Chromaffin granule-associated phosphatidylinositol 4-kinase activity is required for stimulated secretion. EMBO J. 15, 2094–101.

Williams, M., Kim, K., 2014. From membranes to organelles: emerging roles for dynamin-like proteins in diverse cellular processes. Eur. J. Cell Biol. 93, 267–77. doi:10.1016/j.ejcb.2014.05.002

Yu, H., Schulten, K., 2013. Membrane sculpting by F-BAR domains studied by molecular dynamics simulations. PLoS Comput. Biol. 9, e1002892. doi:10.1371/journal.pcbi.1002892

Yu, X., Cai, M., 2004. The yeast dynamin-related GTPase Vps1p functions in the organization of the actin cytoskeleton via interaction with Sla1p. J. Cell Sci. 117, 3839–53. doi:10.1242/jcs.01239

Zhao, L., Shi, X., Li, L., Miller, D.J., 2007. Dynamin 2 associates with complexins and is found in the acrosomal region of mammalian sperm. Mol. Reprod. Dev. 74, 750–7. doi:10.1002/mrd.20660

Table 1. Yeast Strains Used in This Study

Strain Number	Strain Name	Source	Genotype
KKY 0002	WT, Yeast Gene Collections (BY4741)	Invitrogen	*MAT a his3Δ1 leu2D met15Δ ura3Δ*
KKY 0248	*vps1*Δ	(Yu and Cai, 2004)	*MAT a ade2-1 trp1-1 can1-100 ura3-52 leu2-3,112 vps1Δ::LEU2 his3-11 15::HIS3*
KKY 0249	*vps1*Δ/Vps1	(Yu and Cai, 2004)	KKY0248 *Vps1-3myc*
KKY 0250	*vps1*Δ/*vps1*^{K42E}	(Yu and Cai, 2004)	KKY0248 *vps1*$^{K42E\text{-}3myc}$
KKY 0251	*vps1*Δ/*vps1*^{S43N}	(Yu and Cai, 2004)	KKY0248 *vps1*$^{S43N\text{-}3myc}$
KKY 0252	*vps1*Δ/*vps1*^{G315D}	(Yu and Cai, 2004)	KKY0248 *vps1*$^{G315D\text{-}3myc}$
KKY 0270	vps1 *C-term*Δ	This study	*MAT a His3Δ leu2Δ met15Δ ura3Δ Vps1-C-term domain::HIS*
KKY 0343	WT	This study	*MAT α his3Δ uraΔ leuΔ trpΔ lysΔ*
KKY 0352	*vps1*Δ	This study	*MAT α his3Δ uraΔ leuΔ trpΔ lysΔ VPS1::KanMx6*
KKY 0484	*vps1*Δ (002)	This study	KKY0002 *VPS1::HIS*
KKY 0751	*vps1*Δ (352) GFP-PH FAPPI	This study	KKY0352 *VPS1::KanMx6 GFP-PH FAPPI*
KKY 1254	Y2HGold	Clontech	*MAT a trp1-901 leu2-3 112 ura3-52 his3-200 gal4Δ gal80Δ LYS2::GAL1 UAS–Gal1 TATA–His3 GAL2 UAS–Gal2 TATA–Ade2 URA3::MEL1 UAS–Mel1 TATA AUR1-C MEL1*

Table 1 continued

Strain Number	Strain Name	Source	Genotype
KKY 1255	Y187	Clontech	*MAT α ura3-5 his3-200 ade2-101 trp1-901 leu2-3 112 gal4Δ gal80Δ met– URA3::GAL1 UAS–Gal1 TATA–LacZ MEL1*
KKY 1272	pGBKT7-Lam	This study	KKY1254 *(pGBKT7-LAM)*
KKY 1273	pGADT7-T	This study	KKY1255 *(pGADT7-T)*
KKY 1274	pGBKT7-53	This study	KKY1254 *(pGBKT7-53)*
KKY 1275	pGBKT7-Vps1	This study	KKY1254 *(pGBKT7-VPS1)*
KKY 1296	pGADT7-Chc1	This study	KKY1255 *(pGADT7-CHC1)*
KKY 1304	pGBKT7-53 x pGADT7-T	This study	KKY1274/KKY1273 (diploid)
KKY 1305	pGBKT7-Lam x pGADT7-T	This study	KKY1272/KKY1273 (diploid)
KKY 1306	pGBKT7-Vps1 x pGADT7-Chc1	This study	KKY1275/KKY1296 (diploid)
KKY 1391	*vps1*Δ/*vps1*^{S43N} GFP-PH FAPPI	This study	KKY0251 *GFP-PH FAPPI*
KKY 1393	*vps1*Δ/*vps1*^{G315D} GFP-PH FAPPI	This study	KKY0252 *GFP-PH FAPPI*
KKY 1395	*vps1*Δ/Vps1 GFP-PH-FAPPI	This study	KKY0249 *GFP-PH FAPPI*
KKY 1400	WT (002) GFP-PH FAPPI	This study	KKY0002 *GFP-PH FAPPI*

Table 1 continued

Strain Number	Strain Name	Source	Genotype
KKY 1402	*vps1*Δ/*vps1*^{K42E} GFP-PH FAPPI	This study	KKY0250 *GFP-PH FAPPI*
KKY 1404	*vps1*Δ (248) GFP-PH FAPPI	This study	KKY0248 *GFP-PH FAPPI*
KKY 1406	vps1 *C-term*Δ GFP-PH FAPPI	This study	KKY0270 *GFP-PH FAPPI*
KKY 1428	pGBKT7-Vps1-GTPase x pGADT7-Chc1	This study	KKY1275 *VPS1-GTPase/* KKY 1296 *CHC1* (diploid)
KKY 1430	pGBKT7-Vps1-MID x pGADT7-Chc1	This study	KKY1275 *VPS1-MID/* KKY1296 *CHC1* (diploid)
KKY 1432	pGBKT7-Vps1-GED x pGADT7-Chc1	This study	KKY1275 *VPS1-GED/* KKY1296 *CHC1* (diploid)
KKY 1438	pGBKT7-Vps1-GTPase	This study	KKY1275 *VPS1-GTPase*
KKY 1439	pGBKT7-Vps1-MID	This study	KKY1275 *VPS1-MID*
KKY 1440	pGBKT7-Vps1-GED	This study	KKY1275 *VPS1-GED*
KKY 1454	pGADT7-Chc1 (1-494)	This study	KKY1296 *CHC1 (1-494)*
KKY 1459	WT (002) Gga1-GFP-HIS	This study	KKY 0002 *GGA1-GFP-HIS*
KKY 1461	*vps1*Δ (352) Gga1-GFP-HIS	This study	KKY 0352 *GGA1-GFP-HIS*
KKY 1466	pGADT7-Chc1 (495-1073)	This study	KKY1296 *CHC1 (495-1074)*

Table 1 continued

Strain Number	Strain Name	Source	Genotype
KKY 1467	pGADT7-Chc1 (1074-1675)	This study	KKY1296 *CHC1 (1074-1675)*
KKY 1468	pGBKT7-Vps1 x pGADT7-Chc1 (1-494)	This study	KKY1275/ KKY1454 (diploid)
KKY 1469	pGBKT7-Vps1-GTPase x pGADT7-Chc1 (1-494)	This study	KKY1438/ KKY1454 (diploid)
KKY 1470	pGBKT7-Vps1-MID x pGADT7-Chc1 (1-494)	This study	KKY 1439/ KKY1454 (diploid)
KKY 1471	pGBKT7-Vps1-GED x pGADT7-Chc1 (1-494)	This study	KKY 1440/ KKY1454 (diploid)
KKY 1472	pGBKT7-Vps1 x pGADT7-Chc1 (495-1073)	This study	KKY1275/ KKY1466 (diploid)
KKY 1473	pGBKT7-Vps1-GTPase x pGADT7-Chc1 (495-1073)	This study	KKY1438/ KKY1466 (diploid)
KKY 1474	pGBKT7-Vps1-MID x pGADT7-Chc1 (495-1073)	This study	KKY 1439/ KKY1466 (diploid)
KKY 1475	pGBKT7-VPS1-GED x pGADT7-Chc1 (495-1073)	This study	KKY 1440/ KKY1466 (diploid)
KKY 1476	pGBKT7-Vps1 x pGADT7-Chc1 (1074-1654)	This study	KKY1275/ KKY1467 (diploid)
KKY 1477	pGBKT7-Vps1-GTPase x pGADT7-Chc1 (1074-1654)	This study	KKY1438/ KKY1467 (diploid)

Table 1 continued

Strain Number	Strain Name	Source	Genotype
KKY 1478	pGBKT7-Vps1-MID x pGADT7-Chc1 (1074-1654)	This study	KKY 1439/ KKY1467 (diploid)
KKY 1479	pGBKT7-Vps1-GED x pGADT7-Chc1 (1074-1654)	This study	KKY 1440/ KKY1467 (diploid)
KKY 1554	*vps1*Δ (484) mRFP-Sft2	This study	KKY0484 *mRFP-SFT2*
KKY 1555	WT (343) mRFP-Sft2	This study	KKY0343 *mRFP-SFT2*
KKY 1557	Gga1-GFP-HIS (002) mRFP-Vps1 full length	This study	KKY 1459 *mRFP-VPS1-full length*
KKY 1558	Gga1-GFP-HIS (352) mRFP-Vps1 full length	This study	KKY 1461 *mRFP-VPS1-Full length*
KKY 1559	Gga1-GFP-HIS (352) mRFP-Vps1-N-terminal	This study	KKY 1461 *mRFP-VPS1-N-terminal*
KKY 1560	Gga1-GFP-HIS (352) mRFP-Vps1-MID	This study	KKY 1461 *mRFP-VPS1-MID*
KKY 1561	Gga1-GFP-HIS (352) mRFP-Vps1-GED	This study	KKY 1461 *mRFP-VPS1-GED*
KKY 1562	Gga1-GFP-HIS (002) mRFP-Vps1-N-terminal	This study	KKY 1459 *mRFP-VPS1-N-terminal*
KKY 1563	Gga1-GFP-HIS (002) mRFP-Vps1-MID	This study	KKY 1459 *mRFP-VPS1-MID*
KKY 1564	Gga1-GFP-HIS (002) mRFP-Vps1-GED	This study	KKY 1459 *mRFP-VPS1-GED*
KKY 1593	Gga1-GFP-HIS (002) mRFP-Vps1-MID+GED	This study	KKY 1459 *mRFP-VPS1-MID+GED*

Table 1 continued

Strain Number	Strain Name	Source	Genotype
KKY 1594	Gga1-GFP-HIS (352) mRFP-Vps1 (MID+GED)	This study	KKY 1461 *mRFP-VPS1-MID+GED*

Table 2: Bacterial Plasmids Used in This Study

Plasmid number	Plasmid name	Source
KKD 0008	GFP-HIS	(Longtine et al., 1998)
KKD 0044	GFP-PH FAPP1	(Stefan et al., 2002)
KKD 0056	DsRed-FYVE-LEU	(Odorizzi et al., 1998)
KKD 0079	pGBKT7-Vps1	This study
KKD 0083	pGADT7	Clontech
KKD 0085	pGADT7-T	Clontech
KKD 0099	pGBKT7	Clontech
KKD 0100	pGBKT7-53	Clontech
KKD 0101	pGBKT7-Lam	Clontech
KKD 0104	pGADT7-Chc1	This study
KKD 0128	pGBKT7-Vps1-MID	This study
KKD 0130	pGBKT7-Vps1-GED	This study
KKD 0134	pGBKT7-Vps1-GTPase	This study
KKD 0143	mRFP-Cps1	(Obara et al., 2013)
KKD 0149	pGADT7-Chc1 (1-494)	This study

Table 2 continued

Plasmid number	Plasmid name	Source
KKD 0150	pGADT7-Chc1 (1074-1654)	This study
KKD 0152	pGADT7-Chc1 (495-1074)	This study
KKD 0190	mRFP-Vps1	This study
KKD 0191	mRFP-Sft2	This study
KKD 215	mRFP-Vps1-GTPase	This study
KKD 217	mRFP-Vps1-MID	This study
KKD 219	mRFP-Vps1-GED	This study
KKD 244	mRFP-Vps1-MID+GED	This study

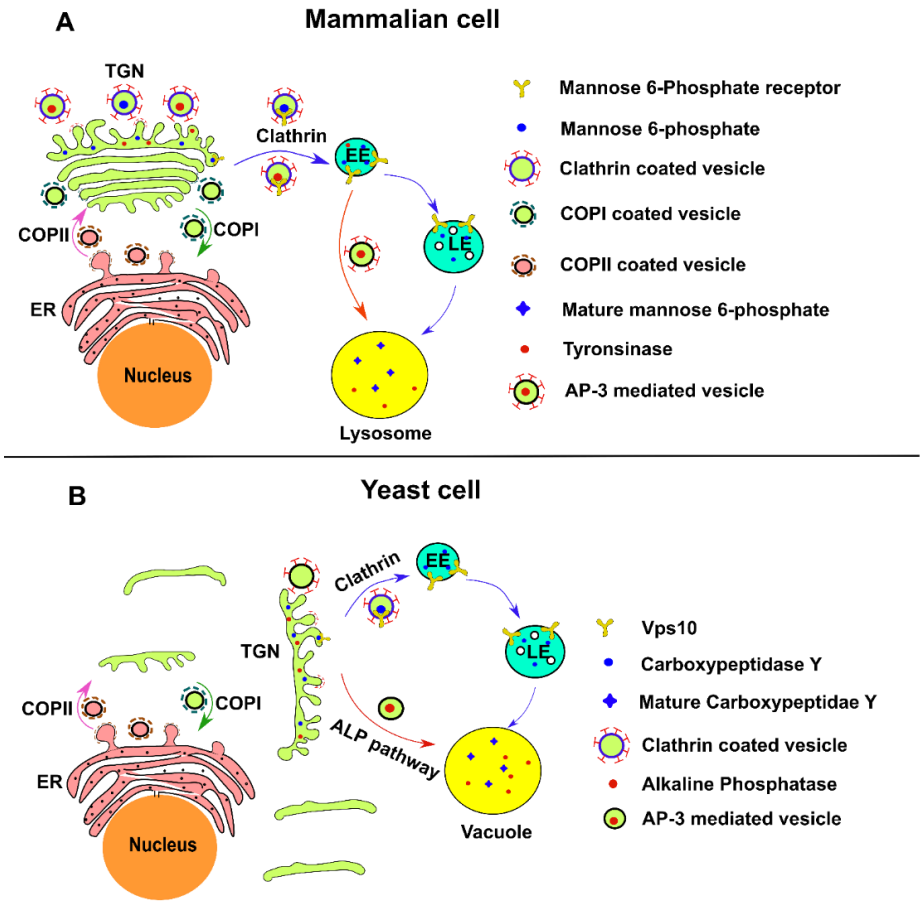

Figure 1: Secretory pathway in Mammalian and Yeast *(S. cerevisiae)* cells.
A. The morphology of the Golgi apparatus and the trafficking of newly synthesized proteins (cargo) to the lysosome in the mammalian cell. These cargoes are transported from the ER to the Golgi apparatus via COPII-coated vesicles (Pink arrow). The TGN-to-lysosome traffic is mediated either by the regular endosomal pathway (Blue arrows) or by AP-3 mediated pathway (Red arrow) from the early endosome to the lysosome. The endosomal pathway transports cargoes including Mannose-6-phosphate receptor (M6PR) toward the endosome via clathrin-coated vesicle. After cargo delivery, the cargo receptor is recycled back to the TGN for the further round of cargo transport. The early endosome that eventually matures into late endosome fuses with the lysosome and transports its content into the lumen of the lysosome. On the other hand, Golgi-derived vesicle containing the cargo tyrosinase follows the AP-3 mediated pathway that bypasses late endosomes for the further process. **B.** In yeast, the Golgi apparatus is dispersed throughout the cytoplasm. Similar to mammals, yeast have two pathways for the transportation of the vacuolar proteins towards the vacuole from TGN either via CPY pathway or by ALP pathway. The CPY pathway is similar to M6PR pathway in mammals. CPY and its receptor Vps10 are delivered to the early endosome, and then to the vacuole via multivesicular bodies/late endosome. However, AP-3 mediated transport/alkaline phosphatase transport starts at TGN and these AP-3 vesicles are transported directly to the vacuole, skipping the endosomal pathway for the further process.

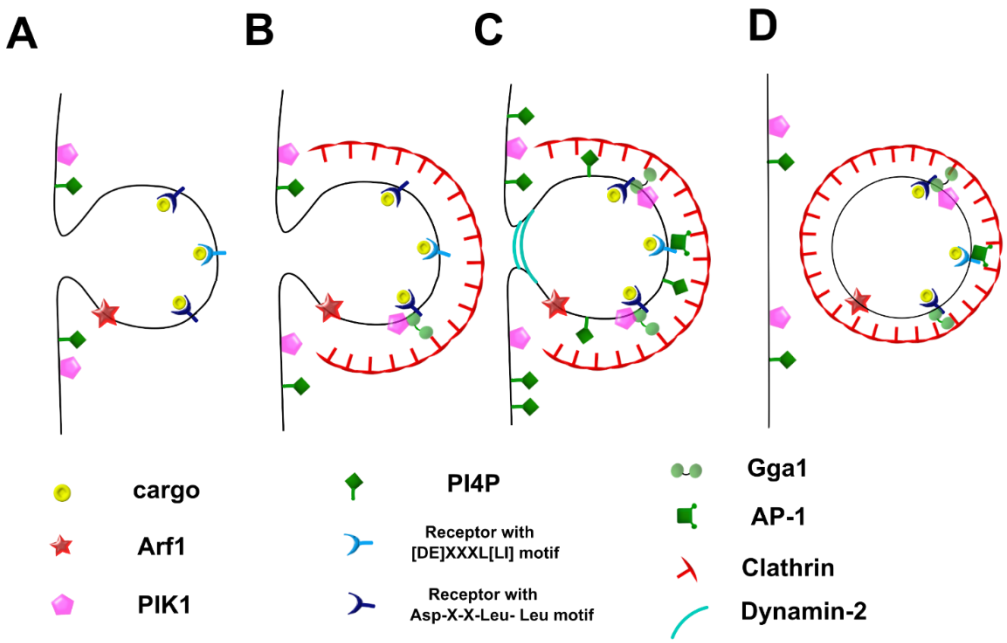

Figure 2: Cargo sorting and the formation of clathrin-coated vesicles at the trans-Golgi network (TGN) **A.** At the TGN, Clathrin-coat assembly is activated by the recruitment of ARF1 to the membrane. ARF1 in turn recruits phosphatidylinositol-4-kinase (PIK1), which initiates low level of phosphatidylinositol-4-phosphate (PI4P) production. **B.** These ARF1 and PI4P stimulate the recruitment of Gga1 adaptor protein that interacts with the specific cargo receptor containing Asp-X-X-Leu-Leu motif and also with the coat protein clathrin, which is recruited at the same time as of the Gga1 adaptor protein (Daboussi et al., 2012). Gga1 also interacts with and stabilizes PIK1 at the TGN, promoting the PI4P production (Daboussi et al., 2012). **C.** Increased PI4P production stimulates recruitment of the additional Gga1 adaptor proteins. In addition, adaptor protein 1 (AP-1) recruitment to the TGN depends on the presence of ARF1. This AP-1 at the TGN binds to the cargo receptor containing [DE]XXXL[LI] motif. After the formation of the clathrin coat and the recruitment of the necessary proteins, Dynamin -2 pinches off the clathrin-coated vesicles. **D.** Clathrin coated vesicles containing cargoes are heading towards the endosome.

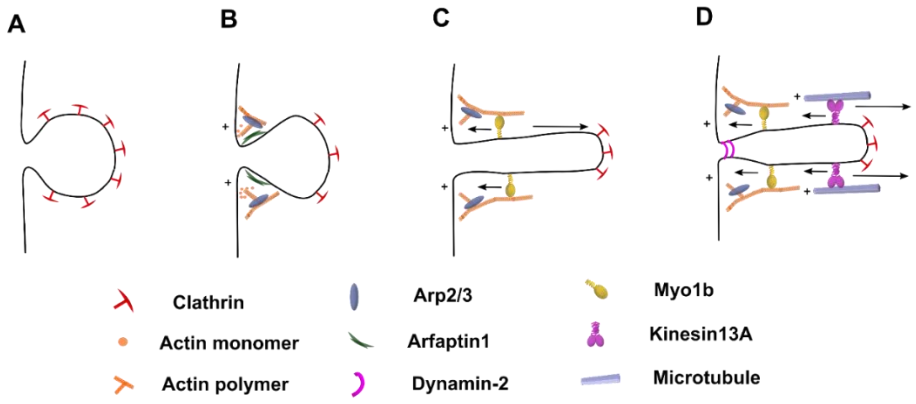

Figure 3: Membrane tubulation at the trans-Golgi network (TGN).
A. Clathrin coat assembly together with accessory proteins induces membrane curvature at the TGN. **B.** Along with the clathrin, actin polymerization supplies the necessary force required for the membrane deformation. Bar domain proteins, Arfaptin-1, binds to the membrane and sustains Arp2/3- mediated actin polymerization towards the membrane. This provides the pushing force required for the tubulation of the membrane. **C.** In addition, Myo1b, which is a plus end directed motor protein (small arrows), upon exertion of power stroke, results in the elongation of the membrane (large arrows) (Almeida et al., 2011). **D.** During the later stages, motor protein, kinesin13A linked to the microtubules (Delevoye et al., 2009) exerts the similar pulling force on the membrane as the actin motor leading to the membrane tubulation. Finally, Dynamin-2 mediates the scission process upon GTP hydrolysis.

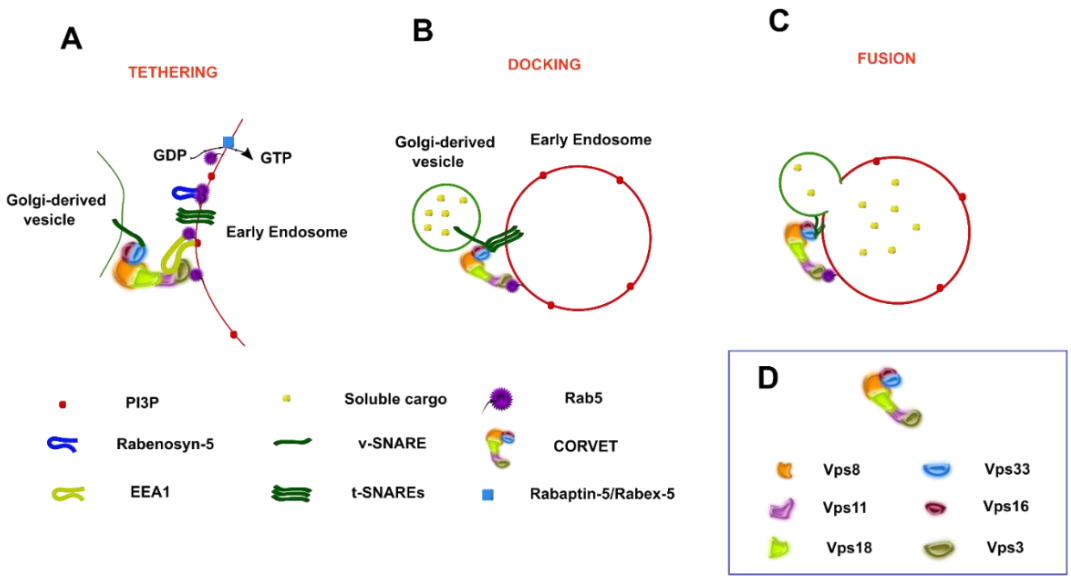

Figure 4: Transport vesicle tethering, docking, and fusion at the early endosome. **A.** Tethering: The CORVET and the Rab effectors mediate tethering of Golgi-derived vesicles with the early endosome. Tethering process is initiated by the activation of the Rab, which is achieved by the GEF, a complex made of Rabaptin-5 and Rabex-5. These Rabs will then recruit CORVET complex and Rab effectors early endosome antigen 1 (EEA1)/Vac1 and SM protein containing complex Rabenosyn-5/Vps45. The CORVET complex associates with SNAREs on the Golgi-derived vesicle and it interacts with Rab5 on the early endosome. **B.** Docking: CORVET utilizes its SNARE-chaperoning activity to capture SNAREs and induces formation of a hetero-tetrameric *trans*-SNARE complex. **C.** Fusion: After the formation of the *trans*-SNARE complex, the Golgi-derived vesicle fuses with the early endosome and releases its content into the lumen of the early endosome. **D.** Subunits of the CORVET complex.

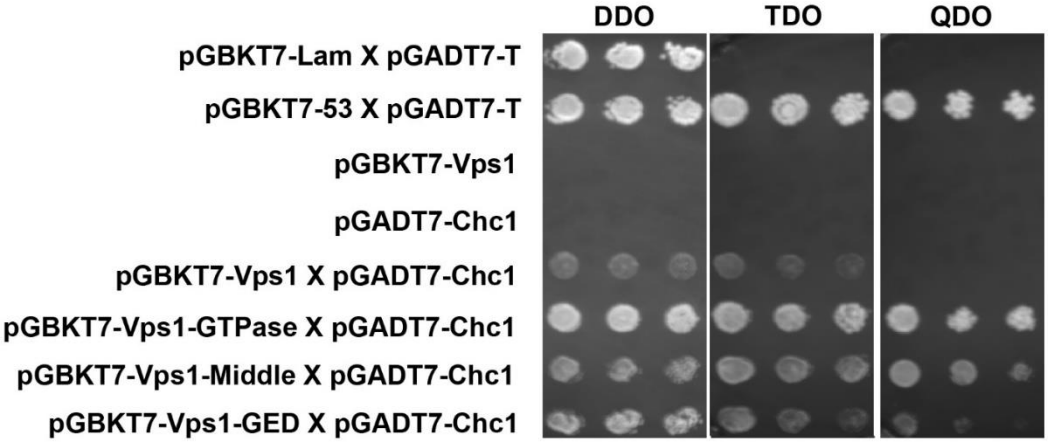

Figure 5: Physical interaction of Vps1 and three domains of Vps1 with Chc1. For a positive control, cells expressing BD-p53 and AD-SV40 large T antigen (KKY 1304) was utilized; p53 was inserted into the bait vector (pGBKT7) (KKY 1274) and SV40 large T antigen into the prey vector (pGADT7) (KKY 1273). Cells expressing BD-Lamin and AD-SV40 large T antigen (KKY 1305), which do not bind to each other, served as the negative control. Cells expressing only either the bait (BD-Vps1) (KKY 1275) or the prey vector (AD-Chc1) (KKY 1296) served as another set of negative controls. Following the same method, the full length of Vps1 and three domains of Vps1 were inserted into the bait vector and Chc1 was inserted into the prey vector. Growth of strains on DDO plates confirmed that those strains contained both bait and prey vectors with corresponding genes of interest. Cells expressing Vps1 and Chc1 (KKY 1306) grew on TDO, indicating that the protein interaction between Vps1 and Chc1 occurred since a reporter gene responsible for the histidine production was activated, allowing cells to grow in the absence of histidine. Similarly, cells co-expressing Chc1 and a domain of Vps1 (KKY 1428, KKY 1430, and KKY 1432) grew on TDO and QDO, indicating the activation of two reporter genes, histidine and adenine allowing cells to grow in the absence of environment lacking both histidine and adenine.

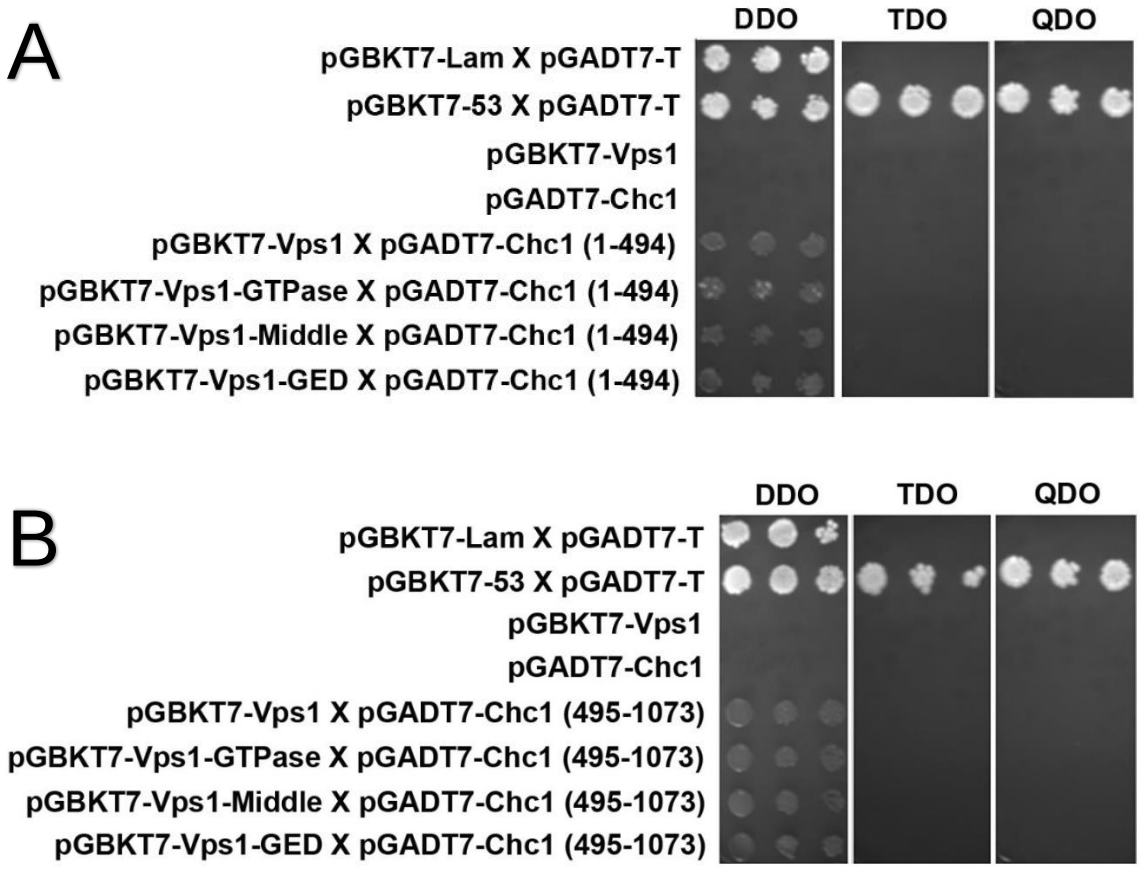

Figure 6: Vps1 does not binds to the N-terminal or the distal-domain of Chc1. **A)** Physical interaction of Vps1 and three domain of Vps1 with Chc1 N-terminal domain and linker consisting of 494 aa. **B)** Physical Interaction of Vps1 and three domain of Vps1 with Chc1 distal domain (495-1073 aa). Diploid cells co-expressing Chc1 N-terminal 494 aa and the full-length Vps1 or its fragment (KKY 1468, KKY 1469, KKY 1470, and KKY 1471) did not grow on TDO or QDO. Similarly, diploid cells co-expressing Chc1 distal domain (495-1073) and each domain of Vps1 (KKY 1472, KKY 1473, KKY 1474, and KKY 1475) did not grow on TDO or QDO, confirming the absence of activation of the reporter genes, histidine and adenine.

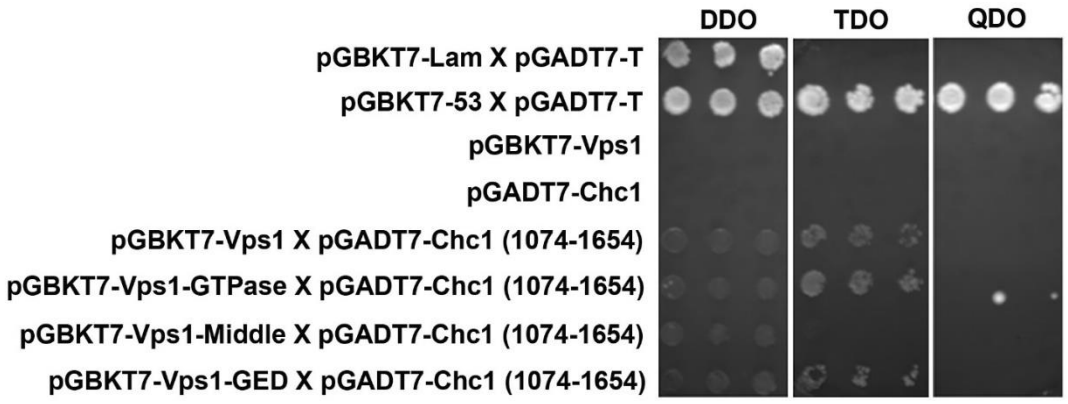

Figure 7: Vps1 binds to the C-terminal 581 aa (1074-1654aa) of Chc1 that contains a proximal domain and a trimerization domain. Diploid cells co-expressing the C-terminal 581 aa of Chc1 and Vps1 (KKY 1476), GTPase domain of Vps1 (KKY 1477), and GED domain of Vps1 (KKY 1479) showed growth on TDO plate, indicating the protein interaction resulting in the activation of the histidine reporter gene.

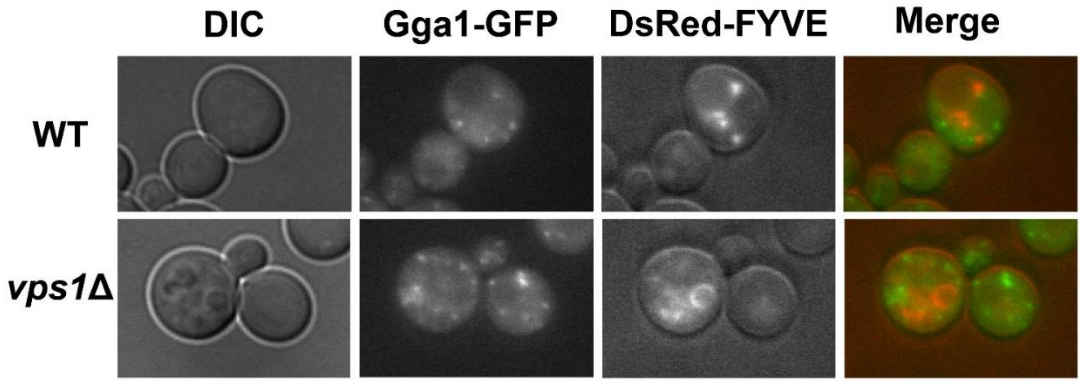

Figure 8: Subcellular localization of Gga1-GFP. To check whether Gga1 is mistargeted to the endosome, Gga1-GFP was expressed in WT (KKY 1459) and *vps1*Δ cells (KKY 1461). Gga1-GFP did not show any co-localization with the DsRed-FYVE, indicating that localization of the Gga1-GFP was not affected by the loss of Vps1.

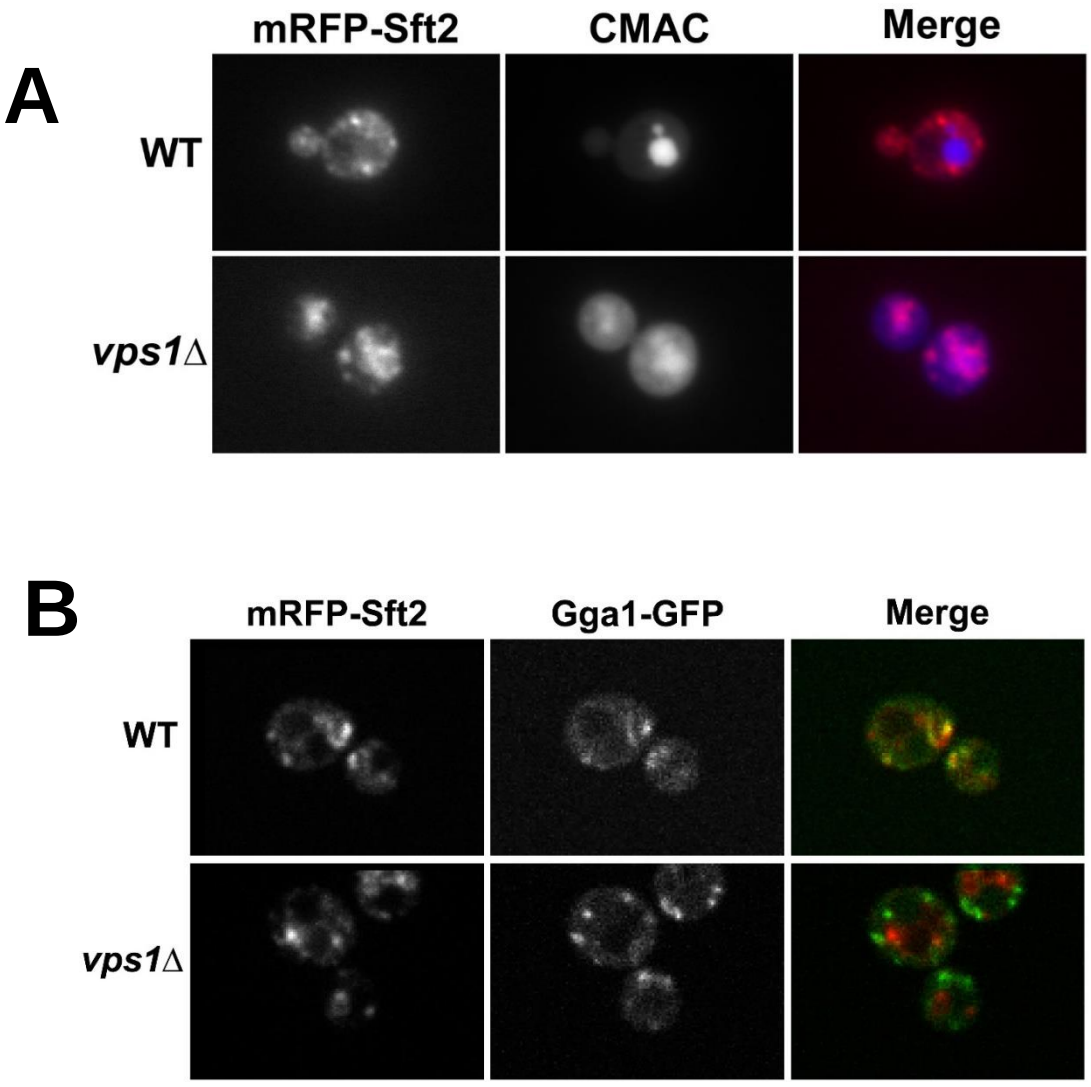

Figure 9: Mislocalization of a late Golgi marker Sft2 to the vicinity of the vacuole in *vps1*Δ cells. **A)** Representative images of WT and *vps1*Δ cells, which were engineered to express mRFP-Sft2 and were stained by CMAC, a dye that labels the rim of the vacuole. **B)** Representative images of WT and *vps1*Δ cells that co-express mRFP-Sft2 and Gga1-GFP. No colocalization of the Golgi marker Gga1-GFP with mRFP-Sft2.

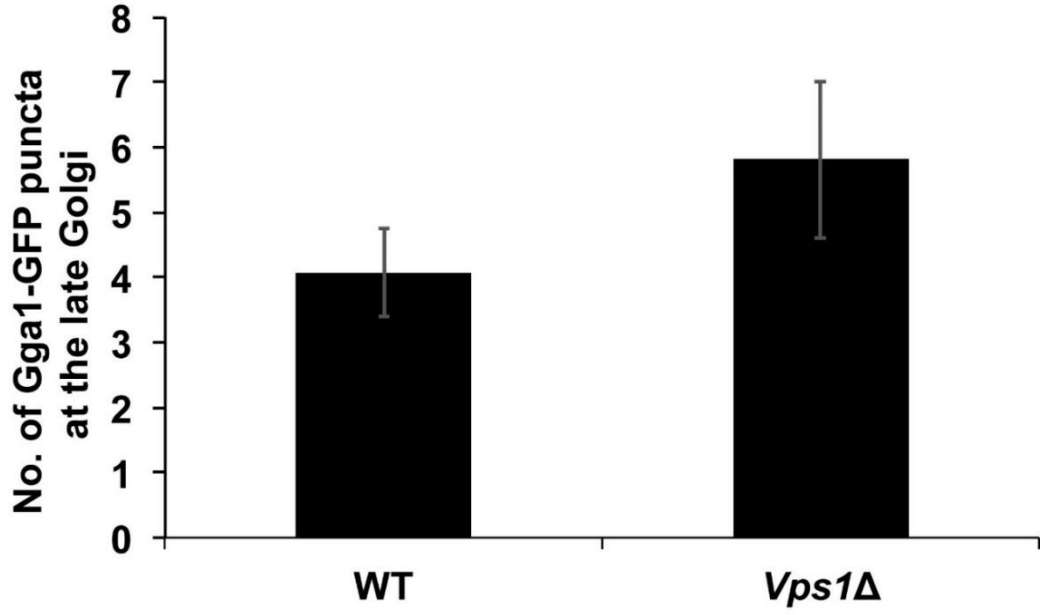

Figure 10: Quantitation of Gga1-GFP puncta in WT and *vps1*Δ cells. The analysis of average number of Gga1-GFP puncta in WT cells is 4.07±0.67, while the average number of Gga1-GFP puncta in *vps1*Δ cells is 5.8±1.20. Shown is the average of three trails (n=30 cells).

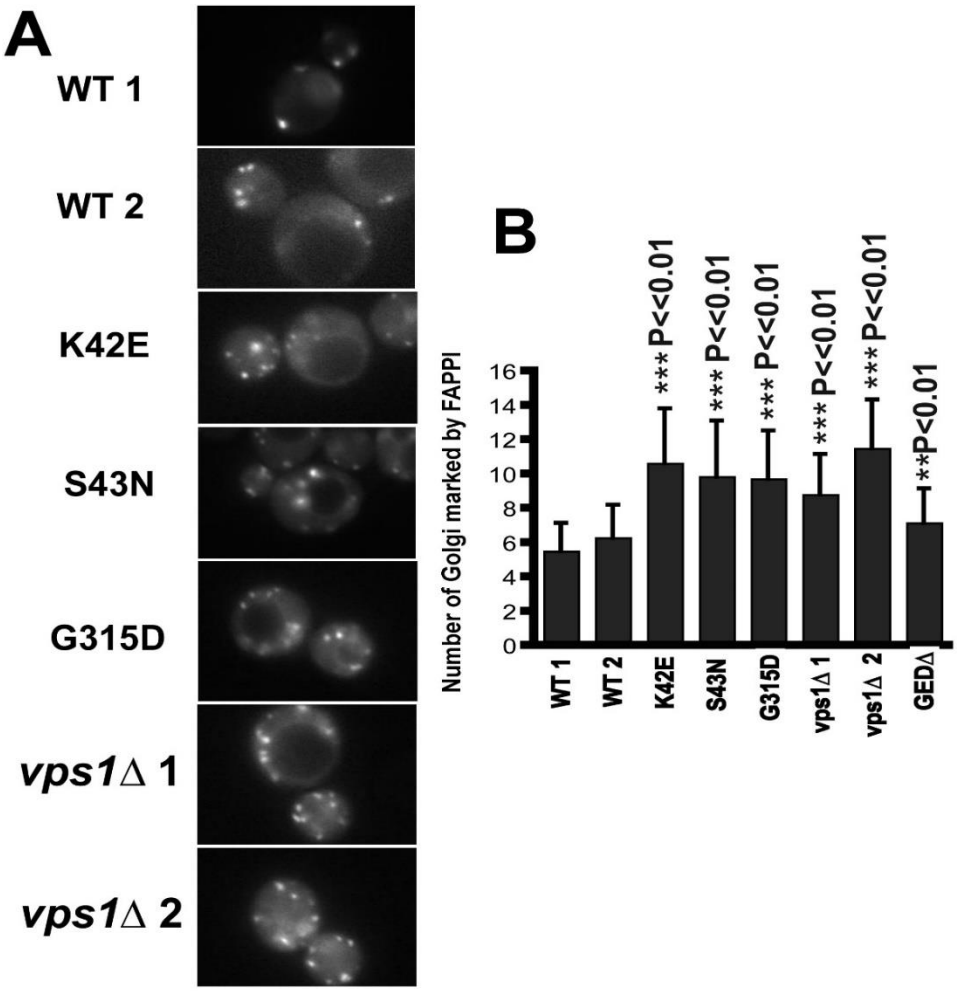

Figure 11: Increase in the number of the late Golgi in *vps1*Δ and *vps1* mutant cells. **A)** Representative images of WT, *vps1*Δ, and *vps1* mutant cells expressing GFP-PH FAPPI (KKY 0751, KKY 1391, KKY 1393, KKY 1395, KKY 1400, KKY 1402, KKY 1404, and KKY 1406) in a single focal plane. **B)** Quantitative analysis data of the number of the late Golgi in WT, *vps1*Δ, and *vps1* mutant cells. The mean Golgi number in WT is 5-6, while the numbers of Golgi in *vps1*Δ and *vps1* GTPase mutant cells ($vps1^{K42E}$, $vps1^{S43N}$, *and* $vps1^{G315D}$) are robustly increased, up to 12 in average. We counted 100 cells for each strain and did 3 experiments to get the average number of Golgi puncta. *** represents p value <0.01, ** represent p value <0.05.

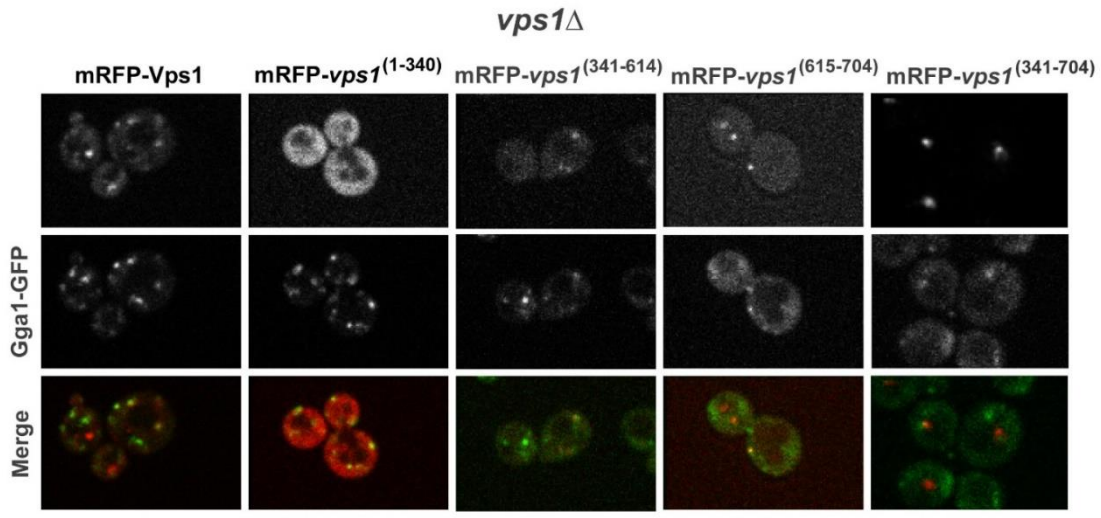

Figure 12: Colocalization of Vps1 and its fragments with Gga1-GFP at the late Golgi. Shown are the representative images that reveal the spatial overlapping of mRFP-Vps1 and its fragments with the Golgi marked by Gga1-GFP.

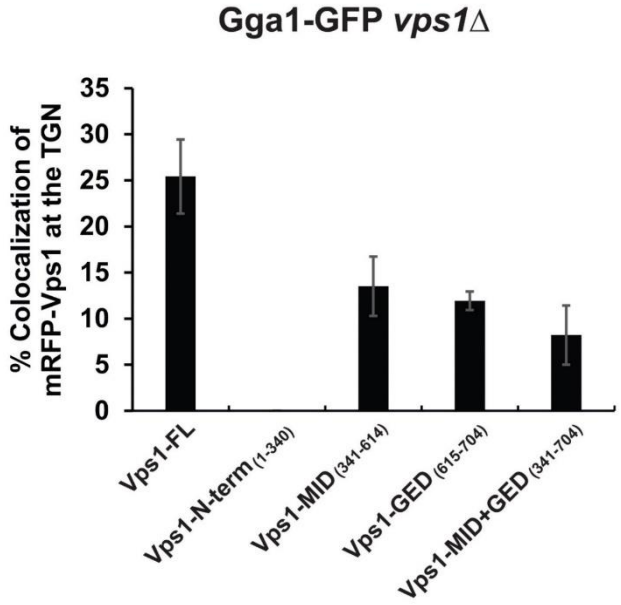

Figure 13: Quantitation analysis of the percentage co-localization of Vps1 and its fragments with Gga1-GFP. The full length of Vps1 showed an average colocalization percentage of 25.4 % (± 4.0), whereas, MID, GED, and MID+GED domains of Vps1 showed 13.55 % (± 3.2), 11.9 % (± 1.0), and 8.21% (± 3.21), respectively. This data indicates that the efficiency for the targeting of the MID, GED, and MID+GED domains of Vps1 was reduced by ~50% when compared with that of full length Vps1. Shown is the average of three trials (n = 30 cells).